**University of Alberta**

# Modeling Rogue Waves with the Kadomtsev-Petviashvili Equation

by

Randy Kanyiri Wanye

A thesis submitted to the Faculty of Graduate Studies and Research
in partial fulfillment of the requirements for the degree of

Master of Science
in
Applied Mathematics

Department of Mathematical and Statistical Sciences


Spring 2012
Edmonton, Alberta

Dedicated to my parents, siblings, friends and family for all their support and encouragement

# Abstract

In this thesis, we will study singular solutions of the Kadomtsev-Petviashvili equation

$$(u_t + 6uu_x + u_{xxx})_x + 3\alpha^2 u_{yy} = 0,\ \alpha^2 = \pm 1$$

that will help improve our understanding and if possible give indicators to the occurrence of rogue waves. We will only study the nonlinear interaction of two such solutions.

## Acknowledgements

Many thanks to my supervisors Drs. Ion Bica(Sept. 2009 to Dec. 2011) and Xinwei Yu (Aug. 2011 to Dec. 2011), and my former supervisor Dr. Mikhail Kovalyov (Sept. 2009 to June 2011) for the help and guidance they provided me during the time of my research on this thesis topic.

# Table of Contents

# List of Figures

# Chapter 1

# Introduction

Rogue waves, also called giant or freak waves, are relatively powerful ocean surface waves that are a threat to large ships and ocean liners. They are responsible for the loss of many ships and lives.

Rogue waves are particularly spontaneous, as they appear from nowhere. That is because they appear from an internal process of energy accumulation sometimes combined with external processes of energy accumulation such as the wind. As spontaneous as they are, they are not totally random, they appear more frequently in certain regions of the ocean than others. These regions seem to have the right ingredients for the internal energy to build up and create rogue waves. One such region is in the area near Cape Agulhas. The Agulhas current runs southwest while the dominant winds are westerlies.

Rogue waves appear mostly in three categories: as walls of water, sets of three called "three sisters" (three sisters is reported to have occurred in Lake Superior), and as single, giant waves that build up and quadruples the height of a new wave formed.

For years, sailors and other eyewitnesses have recounted their encounters with large monstrous waves. These stories have been dismissed by oceanographers. However, this attitude changed following the scientific measurement of a large wave, called the “Draupner wave” at the Draupner platform, in the North Sea on January 1, 1995. Since then, several other accounts of rogue waves have been given, mostly in the media.

Even if we cannot determine all the factors that create a rogue wave, causes may include strong winds together with fast converging currents, or diffractive focusing of winds and currents. Another cause may be a prominent nonlinear effect in which a particular type of nonlinear wave forms and extracts energy from other nonlinear waves, growing into a bigger and taller wave. The different causes that create rogue waves give rise to the occurrence of different types. The common elements in their occurrence are the associated elevations and depressions of the surrounding water.

There are several models for rogue waves. Some scientists tried to model them using the nonlinear Schrödinger equation (see ‘How to excite rogue waves’, N. Akhmediev et. al.). Other models used data collected on the heights of waves. However, none of these models are satisfactory because they don’t give a complete picture of rogue waves.

Here are pictures of rogue waves curled from the Internet below. Figures 1.1 and 1.2 are found at http://justcoolpics.blogspot.com/2010/04/surfing-giant-waves.html and http://earthsky.org/earth/lev-kaplan-rogue-waves-are-not-tsunamis respectively.

Figure 1.1: An example of a rogue wave - 1

Figure 1.2: An example of a rogue wave - 2

## 1.1 Objective

In this thesis, we will try to understand the basic mechanism of the rogue wave. Rogue waves are a localized phenomenon both in space and in time, most frequently occurring far out at sea. We will make use of the equation derived by Kadomtsev and Petviashvili

$$(u_t + 6uu_x + u_{xxx})_x + 3\alpha^2 u_{yy} = 0, \quad \alpha^2 = \pm 1 \tag{1.1}$$

and named after them, the Kadomtsev-Petviashvili equation (KP equation), which is one of the many models for water waves. The evolution of the waves described by (1.1) is weakly nonlinear, weakly dispersive and weakly two-dimensional. The sign of $\alpha^2$ depends on the magnitudes of gravity and surface tension. When $\alpha^2 = -1$, surface tension dominates gravity (gravity is negligible) and (1.1) is known as the KPI equation. When $\alpha^2 = 1$, gravity dominates surface tension (surface tension is negligible) and (1.1) is known as the KPII equation.

The KP equation (1.1) has been widely studied and used in the description of several interesting phenomena. However, much of the interest in these nonlinear evolution equations is due to the fact that they are *completely integrable systems*. The initial value problem for each of these equations is solved by a method called *Inverse Scattering Transform*.

We will consider appropriate singular solutions of the KP equation, and study whether through their nonlinear interaction they can create rogue waves. The KP equation will not be able to fully describe this phenomenon due to its limitations, which includes the equation not accounting for overturning waves. However, we will show that despite it's limitations, it gives a good explanation to how rogue waves occur.

## 1.2 Problem Statement

With giant waves like rogue waves occurring and causing the loss of many ships and lives, a good understanding of their occurrence will be of great help. Rogue waves are not tsunamis, which are set in motion by earthquakes and propagate at high speeds, building up as they get to the shore. Rogue waves occur most frequently in deep water and are short-lived.

We attempt to improve the understanding and if possible the prediction in the occurrence of these waves by using the Kadomtsev-Petviashvili equation. This will be made possible by focusing on one of the many causes of these waves, the nonlinear effects. Thus, we study solutions of the KP equation.

The organization of this thesis is as follows: in Chapter 1 we give an overview of our study, state the objective and introduce the problem. In Chapter 2 the physical derivation of the KP model is thoroughly presented. The main results of this thesis are presented in Chapter 3, here special solutions of the KP equation are given and we will see that these solutions give an idea to the study of rogue waves in Section 3.3. In Sections 3.2 and 3.3, singular waves and the superposition of two singular wave solutions are presented. We conclude the thesis in Chapter 4, by discussing the results and some of their properties.

# Chapter 2

# The Kadomtsev-Petviashvili Equation; Physical Derivation, $N$-Soliton Wall Solution

Before we give the physical derivation of the KP equation, here is a small introduction to solitary waves and solitons.

John Scott Russell made an important discovery concerning the water wave problem in 1844, a phenomenon he termed *solitary wave*. This discovery gave birth to the modern study of solitons.

From Russell's observation, we find that the solitary wave has the following properties

1. permanent form
2. velocity of propagation given by $c^2 = g(h + a)$[i]
3. taller waves travel faster than shorter ones

[i] where $g$, $h$ and $a$ are acceleration due to gravity, uniform depth, and amplitude as measured from an undisturbed level respectively

Unfortunately, Russell's observations contradicted Airy's shallow water theory that waves of finite amplitude do not propagate without change of profile.

Russell's work on the solitary wave received scientific importance and was mathematically explained separately by Boussinesq and Rayleigh (1870), using the equations of motion for an inviscid incompressible fluid. They found Russell's equation for the velocity of propagation. They also showed that the wave profile $z = \zeta(x,t)$ for the free surface elevation is

$$\zeta = a\,\mathrm{sech}^2\frac{x-ct}{\lambda}, \;\; \varepsilon = \frac{a}{h} \ll 1, \;\; \delta^2 = \left(\frac{h}{h}\right)^2 = O(\varepsilon) \tag{2.1}$$

where $a$ and $\lambda$ are the characteristic amplitude and wavelength respectively in the $x$-direction. The characteristic wavelength $\lambda$ is determined by the Ursell number

$$U = \frac{3\varepsilon}{4\delta^2} = 1 \tag{2.2}$$

This Ursell number tells us that the essential quality of the solitary wave is the balance between nonlinearity and dispersion, [26].

For more detailed discussions on solitary waves and solitons, see [1], [7] or [24].

## 2.1 Physical Derivation of the KP Equation

In this section, we derive the model equation describing the surface water problem in a weakly two-dimensional space plus time. Kadomtsev and Petviashvili (1970), derived the equation, now named after them, to model the evolution of long ion-acoustic waves of small amplitude propagating in plasmas under the effect of long transverse perturbations.

The KP equation models shallow water waves where the amplitude of the wave $a$ must be less than the undisturbed depth $h$ with respect to the horizontal $(x, y)$ wavenumber $(k, m)$ of the characteristic disturbances and $g$ is acceleration due to gravity, [26]. The original KP equation is of the form

$$\left(\frac{1}{\nu_0}\zeta_t + \zeta_x + \frac{3}{2h}\zeta\zeta_x + \frac{h^2}{6}\zeta_{xxx}\right)_x + \frac{1}{2}\zeta_{yy} = 0, \ \ \nu_0 = \sqrt{\frac{g}{h}} \qquad (2.3)$$

where $\zeta(x, y, t)$ is the wave profile for the free surface elevation. Equation (2.3) was derived based on the following assumptions:

1. $\frac{a}{h} \ll 1$, small amplitude
2. $h^2(k^2 + m^2) \ll 1$, long waves
3. $\frac{m}{k} \ll 1$, nearly one-dimensional.

We derive the physical KP equation by assuming that the amplitude $a$ of oscillation of the free surface and the ratio of amplitude to wavenumber are small. This implies that the slope of the surface is small, and that the instantaneous depth does not differ significantly from the undisturbed depth. These conditions will allow us to linearize the problem, [18].

The classical water wave problem considers a fluid that is, [1]

1. incompressible
2. irrotational
3. inviscid
4. homogeneous
5. subject to gravitational acceleration $g$.

A fluid with the above features is usually known as an ideal fluid in fluid mechanics.

We consider a fluid that rests on a horizontal impermeable bed of finite extent at $z = -h$ and has a free surface at $z = \eta(x, y, t)$, $\eta$ represents the elevation of the free surface above some reference plane position $x$,$y$ and time $t$. For a schematic illustration to the derivation of the Kadomtsev-Petviashvili equation for water waves, see Figure 5.1 in [9].

Let $\mathbf{u}$ be the velocity vector of a particle at a point. Since the fluid is incompressible and irrotational, we have that

$$\nabla \cdot \mathbf{u} = 0, \;\; \nabla = \left(\frac{\partial}{\partial x}, \frac{\partial}{\partial y}, \frac{\partial}{\partial z}\right) \tag{2.4}$$

and

$$\nabla \times \mathbf{u} = 0 \tag{2.5}$$

The fluid has a velocity potential $\phi$, such that $\mathbf{u} = \nabla\phi$, and satisfies

$$\nabla^2\phi = 0 \qquad\qquad -h < z < \eta(x, y, t) \tag{2.6}$$

To have a well posed problem, we need to impose boundary conditions at the bottom of the bed and at the free surface.

The normal component of velocity should satisfy

$$\mathbf{u} \cdot \mathbf{n} = 0 \tag{2.7}$$

at the bottom since the bed is impermeable (no penetration). This gives us

$$\frac{\partial\phi}{\partial z} = 0 \qquad\qquad \text{at } \; z = -h \tag{2.8}$$

On the free surface, we have a kinematic boundary condition, that is, the fluid at the boundary flows along the boundary and never leaves,

$$\frac{D\eta}{Dt} \equiv \eta_t + \phi_x \eta_x + \phi_y \eta_y = \phi_z \text{ at } z = \eta \tag{2.9}$$

[ii]

For our problem (small amplitude waves), $\phi_x$, $\eta_x$, $\phi_y$ and $\eta_y$ are small, so $\phi_x \eta_x$, $\phi_y \eta_y$ are negligible. Equation (2.9) then simplifies to

$$\eta_t = \phi_z \qquad \text{at } z = \eta \tag{2.10}$$

Taylor expanding equation (2.10) about $\eta = 0$, we have

$$\frac{\partial \eta}{\partial t} = \frac{\partial \phi}{\partial z}\Big|_{z=0} + \eta \frac{\partial^2 \phi}{\partial z^2}\Big|_{z=0} + \ldots \tag{2.11}$$

which approximates to

$$\frac{\partial \eta}{\partial t} = \frac{\partial \phi}{\partial z} \qquad \text{at } z = 0 \tag{2.12}$$

At $z = \eta$, we have a dynamic boundary condition that involves the interface between water and air (fluid-fluid boundary). On this surface, pressure is not continuous across the interface. There should be a pressure balance

$$\Delta p = T \nabla \cdot \mathbf{n} \tag{2.13}$$

where $\Delta p = p_a - p$ is the change in pressure, $p_a$ is atmospheric pressure, $T$ is surface tension.

[ii] $\frac{D\eta}{Dt} = \frac{\partial \eta}{\partial t} + \mathbf{u} \cdot \nabla \eta$

For an interface with radii of curvature $R_1$ and $R_2$, the pressure jump across the interface is, [18]

$$\Delta p = T\left(\frac{1}{R_1} + \frac{1}{R_2}\right) \qquad \text{at } z = \eta \tag{2.14}$$

where

$$\frac{1}{R_1} = \frac{\eta_{xx}(1+\eta_y^2)}{(1+\eta_x^2+\eta_y^2)^{\frac{3}{2}}} \approx \eta_{xx} \tag{2.15}$$

and

$$\frac{1}{R_2} = \frac{\eta_{yy}(1+\eta_x^2)}{(1+\eta_x^2+\eta_y^2)^{\frac{3}{2}}} \approx \eta_{yy} \tag{2.16}$$

The above approximations are only valid for small slopes. For this, the boundary condition (2.14) becomes

$$p \approx -T(\eta_{xx} + \eta_{yy}) \tag{2.17}$$

where the atmospheric $p_a$ is considered to be zero here, (i.e, $p_a = 0$). Since we have an ideal flow, we can apply the unsteady Bernoulli's equation for small amplitude waves:

$$\frac{\partial \phi}{\partial t} + \frac{p}{\rho} + gz = C(t) \tag{2.18}$$

where $\rho$ is the density of the fluid, $C(t)$ is an integrating function independent of location. Defining $\phi$ as $\phi - \int C(t)dt$, we have

$$\frac{\partial \phi}{\partial t} = -g\eta + S(\eta_{xx} + \eta_{yy}) \qquad \text{at } z = \eta \tag{2.19}$$

where $S = \frac{T}{\rho}$. The term $\frac{\partial \phi}{\partial t}$ in (2.19) can be evaluated at $z = 0$ rather than at $z = \eta$ for small amplitude waves.

The linearized mathematical model describing the surface, small amplitude gravity waves in a weakly two-dimensional space plus time is

$$\nabla^2\phi = 0 \qquad -h < z < \eta(x,y,t) \tag{2.20a}$$

$$\frac{\partial\phi}{\partial z} = 0 \qquad \text{at } z = -h \tag{2.20b}$$

$$\frac{\partial\phi}{\partial z} = \frac{\partial\eta}{\partial t} \qquad \text{at } z = 0 \tag{2.20c}$$

$$\frac{\partial\phi}{\partial t} = -g\eta + S(\eta_{xx} + \eta_{yy}) \qquad \text{at } z = \eta \tag{2.20d}$$

To apply the boundary conditions, we need to assume a form for $\eta(x,y,t)$. Since small-amplitude water waves become roughly sinusoidal some time after their generation, we choose $\eta(x,y,t)$ to be of the form

$$\eta(x,y,t) = e^{i(kx+my-\omega t)} \tag{2.21}$$

Another reason for this choice is that, an arbitrary disturbance can be decomposed into sinusoidal components by Fourier analysis.
Equation (2.21) and the boundary conditions (2.20c) and (2.20d) suggests that we look for a separable solution of equation (2.20) of the form

$$\phi(x,y,z,t) = f(z)e^{i(kx+my-\omega t)} \tag{2.22}$$

where $f(z)$ and $\omega(k,m)$ are to be determined. Substituting equation (2.22) into equation (2.20a), we obtain

$$f'' - \kappa^2 f = 0, \;\; \kappa = \sqrt{k^2+m^2} \tag{2.23}$$

whose general solution is

$$f(z) = C_1 e^{\kappa z} + C_2 e^{-\kappa z}, \;\; C_1, C_2 \;\text{ are constants.} \tag{2.24}$$

The velocity potential is

$$\phi(x, y, z, t) = (C_1 e^{\kappa z} + C_2 e^{-\kappa z}) e^{i(kx+my-\omega t)} \tag{2.25}$$

Using the boundary conditions (2.20b) and (2.20c), we find

$$C_1 = -\frac{i\omega}{\kappa(1 - e^{-2kh})} \tag{2.26}$$

$$C_2 = -\frac{i\omega e^{-2kh}}{\kappa(1 - e^{-2kh})} \tag{2.27}$$

The solution for the velocity potential is then

$$\phi(x, y, z, t) = -\frac{i\omega}{\kappa} \frac{\cosh(\kappa(z + h))}{\sinh(\kappa h)} e^{i(kx+my-\omega t)} \tag{2.28}$$

We solved (2.20a) using only the kinematic boundary conditions (2.20b) and (2.20c), which is typical of irrotational flows. We now apply the dynamic boundary condition (2.20d) to the problem. This gives us a relation for $\kappa$ and $\omega$. Substituting equations (2.28) and (2.21) into (2.20d), we obtain

$$\omega^2 = \kappa(g + S\kappa^2) \tanh(\kappa h) \tag{2.29}$$

A relation such as equation (2.29), giving $\omega$ as a function of $\kappa$ is called a *dispersive relation*, because it expresses the nature of the dispersive process.

If we consider only the positive root of equation (2.29)

$$\omega = \sqrt{\kappa(g + S\kappa^2)\tanh(\kappa h)} \tag{2.30}$$

Taylor expanding equation (2.30) about $\kappa = 0$, we have

$$\omega = \nu_\circ \kappa \left(1 - \frac{1}{6}h^2(1 - \hat{S})\kappa^2\right) + O(\kappa^5) \tag{2.31}$$

$$\text{where} \qquad \nu_\circ = \sqrt{gh}, \;\; \hat{S} = \frac{3S}{gh^2}$$

$\nu_\circ$ and $\hat{S}$ represent the phase speed and the dimensionless surface tension. From equation (2.31), we obtain the group velocity as

$$c = \frac{\omega}{\kappa} = \nu_\circ \left[1 - \frac{1}{6}h^2(1 - \hat{S})\kappa^2\right] + O(\kappa^4) \tag{2.32}$$

This shows that the linearized problem is non-dispersive as $\kappa \to 0$, (i.e, long waves or shallow water waves), where it is weakly dispersive. The KdV and KP equations arise as models of the water wave problem in this weakly dispersive limit $\kappa h \ll 1$, [1].

For sufficiently small $\kappa$, we drop the $O(\kappa^5)$ term, so that equation (2.31) becomes

$$\omega = \nu_\circ \sqrt{k^2 + m^2}\left[1 - \frac{1}{6}h^2(1 - \hat{S})(k^2 + m^2)\right] \tag{2.33}$$

If we assume that the waves are nearly one dimensional, $k$ small but $(m/k)^2 \ll 1$, we have that

$$\frac{1}{\nu_\circ}\omega k - k^2 - \frac{1}{2}m^2 + \frac{1}{6}h^2(1 - \hat{S})k^4 = 0 \tag{2.34}$$

We recall that, we assumed the solution of the linearized problem equation (2.20) to be of the form (2.21). Equation (2.34) suggests that (2.21) satisfies

$$\left(\frac{1}{\nu_\circ}\eta_t + \eta_x + \frac{1}{6}h^2(1-\hat{S})\eta_{xxx}\right)_x + \frac{1}{2}\eta_{yy} = 0 \tag{2.35}$$

To satisfy certain conservation laws from physics and also to cause a variation in the amplitude for both space and time of $\eta(x, y, t)$, we add the nonlinear term $(\eta\eta_x)_x$ to (2.35), thus obtaining

$$\left(\frac{1}{\nu_\circ}\eta_t + \eta_x + \eta\eta_x + \frac{1}{6}h^2(1-\hat{S})\eta_{xxx}\right)_x + \frac{1}{2}\eta_{yy} = 0 \tag{2.36}$$

Under the change of variables

$$r = \frac{x - \nu_\circ t}{h}, \;\; \zeta = \frac{y}{h}, \;\; \tau = \frac{\nu_\circ t}{6h}, \;\; \eta = u(r, \zeta, \tau) \tag{2.37}$$

we have the dimensionless form of equation (2.36)

$$(u_\tau + 6uu_r + (1-\hat{S})u_{rrr})_r + 3u_{\zeta\zeta} = 0 \tag{2.38}$$

For very thin sheets of water $\hat{S} > 1$ (surface tension dominates gravity), then equation (2.38) is equivalent to equation (1.1) in Section 1.1, with $\alpha^2 = -1$, that is

$$(u_t + 6uu_x + u_{xxx})_x - 3u_{yy} = 0 \tag{2.39}$$

which is called the KPI equation. For most cases of interest in water waves $1 - \hat{S} > 0$ (usually, $\hat{S} \ll 1$ and is negligible). This corresponds to $\alpha^2 = 1$ in equation (1.1) of Section 1.1, called the KPII equation, that is

$$(u_t + 6uu_x + u_{xxx})_x + 3u_{yy} = 0 \tag{2.40}$$

## 2.2 $N$-soliton Wall Solution of the KP Equation

In this section, we present the $N$-soliton wall solution for the KP equation. To derive this solution, we will make use of the Dressing Method devised by Zakharov and Shabat, and presented in [21].

### 2.2.1 Lax's Representation

We introduce Lax's representation for solving partial differential equations. This representation is used by Zakharov and Shabat in their Dressing Method. The concept of Lax's representation is reproduced from [1].

Consider two differential operators $L$ and $M$, where $L$ is the operator of the spectral problem

$$L\psi = \lambda\psi \tag{2.41}$$

and $M$ is the operator governing the associated time evolution of the eigenfunction $\psi(x, t)$

$$\psi_t = M\psi \tag{2.42}$$

Taking a time derivative of (2.41) gives

$$L_t\psi + L\psi_t = \lambda_t\psi + \lambda\psi_t \tag{2.43}$$

and using (2.42), we obtain

$$[L_t + (LM - ML)]\psi = \lambda_t\psi \tag{2.44}$$

and in order to solve for the nontrivial eigenfunctions $\psi(x,t)$

$$L_t + [L, M] = 0 \tag{2.45}$$

where

$$[L, M] = LM - ML,$$

if and only if $\lambda_t = 0$. Equation (2.45) is called *Lax's equation*, and contains a nonlinear evolution equation for suitably differential operators $L$ and $M$. For example, for the KdV equation

$$u_t + 6uu_x + u_{xxx} = 0 \tag{2.46}$$

choosing

$$L = \frac{\partial^2}{\partial x^2} + u \tag{2.47}$$

and

$$M = (\alpha + u_x) - (4\lambda + 2u)\frac{\partial}{\partial x} \tag{2.48}$$

equation (2.45) is satisfied.

Equation (2.46) may be thought of as the compatibility condition of the linear operators (2.47) and (2.48). If a nonlinear partial differential equation arises as a result of the compatibility condition of the two operators $L$ and $M$, then (2.45) is called the *Lax representation* of the partial differential equation and the pair $L$ and $M$, written $(L, M)$ are the *Lax pair*.

The following Lax pair, [21] were found for the KP equation (1.1),

$$L = \alpha\frac{\partial}{\partial y} + \frac{\partial^2}{\partial x^2} + u(x, y, t) \tag{2.49}$$

and

$$M = -4\frac{\partial^3}{\partial x^3} - 6u\frac{\partial}{\partial x} - 3u_x + 3\alpha\omega \tag{2.50}$$

The Lax pair (2.49) and (2.50), and the equation (2.45) allow us to write the KP equation in evolution form as

$$u_t - 6uu_x - u_{xxx} - 3\alpha^2\omega_y = 0, \;\; \omega_x = u_y \tag{2.51}$$

which is equivalent to

$$(u_t - 6uu_x - u_{xxx})_x - 3\alpha^2 u_{yy} = 0 \tag{2.52}$$

Since the properties of solutions of the KP depends on the sign of $\alpha^2$, we have different choices of $L$ for each choice of $\alpha$.

For $\alpha^2 = -1$ (KPI equation), $L$ is a nonstationary Schrödinger operator

$$L = i\frac{\partial}{\partial y} + \frac{\partial^2}{\partial x^2} + u(x, y, t) \tag{2.53}$$

and for $\alpha^2 = 1$ (KPII equation), $L$ is the operator of heat conductivity

$$L = \frac{\partial}{\partial y} + \frac{\partial^2}{\partial x^2} + u(x, y, t) \tag{2.54}$$

### 2.2.2 $N$-soliton Wall Solution of the KPII equation

To construct this solution, we use the technique of the Dressing Method in constructing several particular solutions. The Dressing Method is reproduced from [21].

Consider the Fredholm operator $\hat{F}$ depending on $y$ and $t$,

$$\hat{F}\phi(x,y,t) = \int_{-\infty}^{\infty} F(x,z,t,y)\phi(z,y,t)dz \tag{2.55}$$

which admits the triangular factorization

$$1 + \hat{F} = (1+\hat{K}^{+})^{-1}(1+\hat{K}^{-}) \tag{2.56}$$

where $\hat{K}^{+}$ and $\hat{K}^{-}$ are the Volterra operators

$$\hat{K}^{+}\phi(x) = \int_{x}^{\infty} K^{+}(x,z,y,t)\phi(z,y,t)dz \tag{2.57}$$

$$\hat{K}^{-}\phi(x) = \int_{-\infty}^{x} K^{-}(x,z,y,t)\phi(z,y,t)dz \tag{2.58}$$

Assume a differential operator

$$L_0 = \alpha\frac{\partial}{\partial y} + M_0$$

is given, where

$$M_0 = m_0\frac{\partial^n}{\partial x^n} + m_1\frac{\partial^{n-1}}{\partial x^{n-1}} + \cdots + m_n \tag{2.59}$$

with the coefficient $m_i$ functions of $x$, $y$, and $t$.

Suppose that $\hat{F}$ commutates with $L_0$

$$\hat{F}L_0 - L_0\hat{F} = 0 \tag{2.60}$$

and also with $\frac{\partial}{\partial t} - A_0$

$$\left(\frac{\partial}{\partial t} - A_0\right)\hat{F} - \hat{F}\left(\frac{\partial}{\partial t} - A_0\right) = 0, \ \ A_0 = -4\frac{\partial^3}{\partial x^3} \tag{2.61}$$

The operator $L_0$ remains invariant, when the space of $\phi(x)$ is transformed by $1 + \hat{F}$, that is

$$(1 + \hat{F})^{-1}L_0(1 + \hat{F}) = L_0$$

$$\Rightarrow \qquad (1 + \hat{K}^+)L_0(1 + \hat{K}^+)^{-1} = (1 + \hat{K}^-)L_0(1 + \hat{K}^-)^{-1}$$

and

$$(1 + \hat{F})^{-1}\left(\frac{\partial}{\partial t} - A_0\right)(1 + \hat{F}) = \frac{\partial}{\partial t} - A_0$$

$$\Rightarrow \qquad (1+\hat{K}^+)\left(\frac{\partial}{\partial t} - A_0\right)(1+\hat{K}^+)^{-1} = (1+\hat{K}^-)\left(\frac{\partial}{\partial t} - A_0\right)(1+\hat{K}^-)^{-1}$$

Once we obtain $\hat{F}$, we find $\hat{K}^+$ by multiplying $(1+\hat{K}^-)$ to the left of (2.56) and obtain

$$(1 + \hat{K}^-)(1 + \hat{F}) = (1 + \hat{K}^+) \tag{2.62}$$

Assuming $z < x$ leads us to the Gel'fand-Levitan-Marchenko equation

$$K^+(x, z, t, y) + F(x, z, t, y) + \int_x^\infty K^+(x, s, t, y)F(s, z, t, y)ds = 0 \tag{2.63}$$

The new class of solutions of the KPII equation is generated from

$$u(x,y,t) = -2\frac{\partial}{\partial x}K^{+}(x,x,y,t) \tag{2.64}$$

Thus the Dressing Method yields a new class of solutions from already known solutions, [21].

Now we apply the Dressing Method to the KPII equation ($\alpha = 1$), and taking note that $\hat{F}$ commutes with both $L_0$ and $\frac{\partial}{\partial t} - A_0$.

$$L_0\hat{F} - \hat{F}L_0 = 0$$

$$\begin{aligned}\Rightarrow \qquad & \left(\frac{\partial}{\partial y} + \frac{\partial^2}{\partial x^2}\right)\int_{-\infty}^{\infty} F(x,z,y,t)\phi(z,y,t)dz \\ & -\int_{-\infty}^{\infty} F(x,z,y,t)\left(\frac{\partial}{\partial y} + \frac{\partial^2}{\partial z^2}\right)\phi(z,y,t)dz = 0\end{aligned}$$

$$\Rightarrow \int_{-\infty}^{\infty}\left[\frac{\partial F(x,z,y,t)}{\partial y} + \frac{\partial^2 F(x,z,y,t)}{\partial x^2} - \frac{\partial^2 F(x,z,y,t)}{\partial z^2}\right]\phi(z,y,t)dz = 0$$

$$\Rightarrow \frac{\partial F}{\partial y} + \frac{\partial^2 F}{\partial x^2} - \frac{\partial^2 F}{\partial z^2} = 0 \tag{2.65}$$

Similarly for $\frac{\partial}{\partial t} - A_0$, we get

$$\frac{\partial F}{\partial t} + 4\left(\frac{\partial^3 F}{\partial x^3} + \frac{\partial^3 F}{\partial z^3}\right) = 0 \tag{2.66}$$

One simple solution of the system of equations (2.65) and (2.66) is choosing $F$ as

$$F(x,z,t,y) = \sum_{n=1}^{N} C_n(y,t) e^{(p_n x + q_n z)} \tag{2.67}$$

where

$$C_n(y,t) = c_n e^{[(q_n^2 - p_n^2)y - 4(p_n^3 + q_n^3)t]} \tag{2.68}$$

and $p_n, q_n, c_n > 0$, $m,n = 1,2,\cdots,N$.

We seek to solve (2.63) for $K^+$ of the form

$$K^+(x,z,t,y) = \sum_{n=1}^{N} K_n(x,t,y) e^{q_n z} \tag{2.69}$$

Substituting equation (2.69) into (2.63), and using equation (2.67), we obtain

$$\begin{aligned} K_n(x,t,y) \quad + \quad & \sum_{m=1}^{N} K_m(x,t,y) C_n(y,t) \frac{e^{(p_n+q_m)x}}{p_n+q_m} = -C_n(y,t) e^{p_n x} \\ & m,n = 1,2,\cdots,N, \;\; p_n + q_m \neq 0 \end{aligned} \tag{2.70}$$

Let $A = A(x,y,t)$ be an $N \times N$ matrix of (2.68),

$$A_{mn} = \delta_{mn} + C_n(y,t) \frac{e^{(p_n+q_m)x}}{p_n+q_m}, \;\; m,n = 1,2,\cdots,N \tag{2.71}$$

where

$$\delta_{mn} = \begin{cases} 1 & \text{if} \quad m = n \\ 0 & \text{if} \quad m \neq n \end{cases}$$

By Cramer's rule, we find that the solution of equation (2.71) is

$$K_n(x,t,y) = \frac{\det A^{(n)}}{\det A}$$

where $A^{(n)}$ is the matrix obtained from $A$ by replacing its $n$-th column with the elements of $-C_n(y,t)e^{p_n z}$.

The solution $K^+$ of (2.63) is therefore

$$K^+(x,z,t,y) = \frac{1}{\det A}\sum_{n=1}^{N} \det A^{(n)} e^{q_n z} \tag{2.72}$$

We know that,

$$\det A = \sum_{n=1}^{N} A_{mn}(-1)^{m+n}\mathcal{M}_{mn} \tag{2.73}$$

where $\mathcal{M}_{mn}$ is the determinant of the minor matrix obtained by deleting the $m$-th row and $n$-th column of $A$.

Differentiating equation (2.73) with respect to $x$, we have

$$\begin{aligned}\frac{\partial}{\partial x}\det A \qquad &= -\sum_{n=1}^{N} e^{q_n x}\sum_{m\in P_n}(-1)^m A_{1m(1)}A_{2m(2)} \\ &\quad \cdots(-c_{m(n)}(y,t)e^{p_{m(n)}x})\cdots A_{Nm(N)} \\ &= -\sum_{n=1}^{N}\det A^{(n)}e^{q_n x}\end{aligned} \tag{2.74}$$

Hence from equation (2.72), we obtain

$$K^+(x,z,t,y) = \frac{1}{\det A}\left(-\frac{\partial}{\partial x}\det A\right) = -\frac{\partial}{\partial x}\ln\det A \tag{2.75}$$

Now from equations (2.64) and (2.75), we get the new solution of the KPII equation

$$u(x, y, t) = 2\frac{\partial^2}{\partial x^2} \ln \det A \tag{2.76}$$

Equation (2.76) is called the $N$-soliton wall solution. The new class of solutions is derived from the soliton-wall solutions.

By constructing the $N$-soliton solution of the KPII equation, we can easily derive the $N$-soliton solution of the KPI equation, by making the change of variables $y \to iy$, $i^2 = -1$.

Some examples of the $N$-soliton solution of the KP equation are given below.

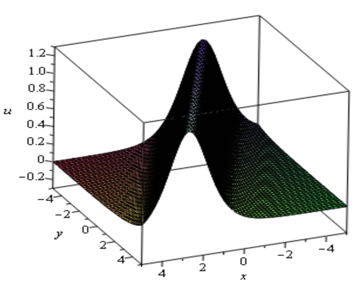

(a) 3D plot

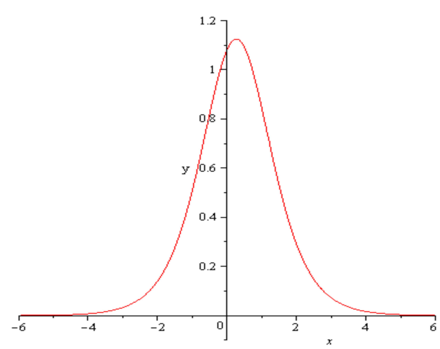

(b) Projection onto $xy$-plane

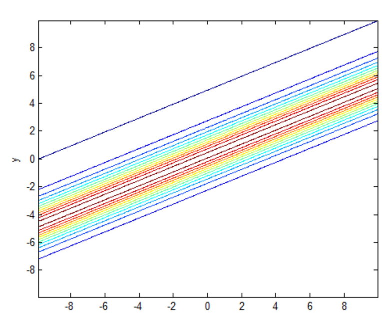

(c) Contour plot

Figure 2.1: 1-soliton wall solution with $p_1 = 1$, $q_1 = 0.5$, $c_1 = 1$, at $t = 0$

Figures 2.1 and 2.2 show a plot of the 1-soliton wall and 2-soliton wall solutions in various views respectively.

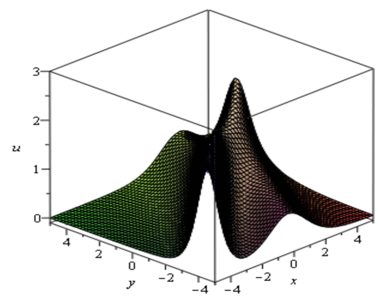


(a) 3D plot

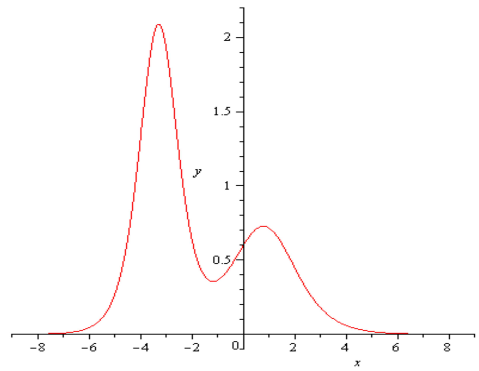


(b) Projection onto $xy$-plane

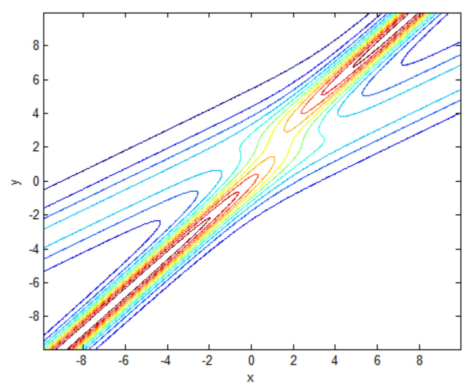


(c) Contour plot

Figure 2.2: 2-soliton wall solution with $p_1 = 1.6$, $p_2 = 0.9$, $q_1 = 0.5$, $q_2 = 0.3$, $c_1 = 2$, $c_2 = 1$, at $t = 0$

# Chapter 3

# Modeling Rogue Waves

## 3.1 Special Solutions of the KP equation

The solution we obtain here is the continuation of the work in [17]. In [17], Kovalyov and Bica derived the $N$-harmonic breather solutions for the KP equation as

$$u(x,y,t) = 2\frac{\partial^2}{\partial x^2}\ln\det\mathcal{K} \tag{3.1a}$$

where $\mathcal{K}$ is an $N\times N$ matrix with entries

$$\mathcal{K} = \begin{pmatrix} K_{11} & K_{12} & \cdots & K_{1N} \\ K_{21} & K_{22} & \cdots & K_{2N} \\ \vdots & \vdots & \vdots & \vdots \\ K_{N1} & K_{N2} & \cdots & K_{NN} \end{pmatrix} \tag{3.1b}$$

$$K_{nn} = -\Upsilon_n + \frac{\cos 2\Gamma_n}{2\lambda_n}, \tag{3.1c}$$

$$K_{nk} = \left[\frac{(\lambda_n+\lambda_k)\cos(\Gamma_n+\Gamma_k)}{\alpha^2(\mu_n-\mu_k)^2+(\lambda_n+\lambda_k)^2} - \frac{(\lambda_n+\lambda_k)\sin(\Gamma_n-\Gamma_k)}{\alpha^2(\mu_n-\mu_k)^2+(\lambda_n-\lambda_k)^2}\right] \quad (3.1d)$$
$$+\alpha\left[\frac{(\mu_n-\mu_k)\sin(\Gamma_n+\Gamma_k)}{\alpha^2(\mu_n-\mu_k)^2+(\lambda_n+\lambda_k)^2} + \frac{(\mu_n-\mu_k)\cos(\Gamma_n-\Gamma_k)}{\alpha^2(\mu_n-\mu_k)^2+(\lambda_n-\lambda_k)^2}\right],$$
$$n \neq k$$

$$\Upsilon_n = \rho_n + x\cos(\alpha\chi_n) + 2\left[\frac{\lambda_n\sin(\alpha\chi_n)}{\alpha} - \mu_n\cos(\alpha\chi_n)\right]y \quad (3.1e)$$
$$+12[\lambda_n^2\cos(\alpha\chi_n) - \alpha^2\mu_n\cos(\alpha\chi_n) + 2\alpha\lambda_n\mu_n\sin(\alpha\chi_n)]t$$

$$\Gamma_n = \gamma_n + \lambda_n x - 2\lambda_n\mu_n y + 4\lambda_n(\lambda_n^2 - 3\alpha^2\mu_n^2)t \quad (3.1f)$$

$$n = 1, 2, \cdots, N$$

where $\lambda_n$'s, $\mu_n$'s, $\chi_n$'s, $\gamma_n$'s, $\rho_n$'s are some appropriately chosen constants. This solution is real whenever the constants $\lambda_n$'s, $\mu_n$'s, $\chi_n$'s, $\gamma_n$'s, $\rho_n$'s are real.

In this thesis, we consider other classes of real solutions of the KP equation, which may be derived just like (3.1) in [17]. These solutions are presented in the theorem below.

**Theorem**[i] **1.** *Let $u(x,y,t)$ be defined as*

$$u(x,y,t) = 2\frac{\partial^2}{\partial x^2}\ln\det\mathcal{K} \quad (3.2)$$

[i]This theorem is based on a suggestion by Dr. Kovalyov (supervisor) to find solutions in terms of sinh and cosh

*where $\mathcal{K}$ is an $N \times N$ matrix given by*

$$\mathcal{K} = \begin{pmatrix} K_{11} & K_{12} & \cdots & K_{1N} \\ K_{21} & K_{22} & \cdots & K_{2N} \\ \vdots & \vdots & \vdots & \vdots \\ K_{N1} & K_{N2} & \cdots & K_{NN} \end{pmatrix} \tag{3.3}$$

1. *Then $u(x, y, t)$ is a solution of the KPI equation if the matrix $\mathcal{K}$ has the following entries*

$$K_{nn} = -\Upsilon_n - \frac{\sinh 2\Gamma_n}{2\lambda_n} \tag{3.4a}$$

$$\begin{aligned} K_{nk} \quad = \quad & \frac{(\lambda_n + \lambda_k)\sinh(\Gamma_n + \Gamma_k)}{(\mu_n - \mu_k)^2 + (\lambda_n + \lambda_k)^2} - \frac{(\lambda_n - \lambda_k)\sinh(\Gamma_n - \Gamma_k)}{(\mu_n - \mu_k)^2 + (\lambda_n - \lambda_k)^2} \\ & + i\left[\frac{(\mu_n - \mu_k)\cosh(\Gamma_n + \Gamma_k)}{(\mu_n - \mu_k)^2 + (\lambda_n + \lambda_k)^2} - \frac{(\mu_n - \mu_k)\cosh(\Gamma_n - \Gamma_k)}{(\mu_n - \mu_k)^2 + (\lambda_n - \lambda_k)^2}\right]^{\text{ii}}, \\ & n \neq k \end{aligned} \tag{3.4b}$$

$$\begin{aligned} \Upsilon_n \quad = \quad & \rho_n + x\cos\chi_n - 2[\lambda_n \sin\chi_n + \mu_n \cos\chi_n]y \\ & - 12[\lambda_n^2 \cos\chi_n - \mu_n^2 \cos\chi_n - 2\lambda_n\mu_n \sin\chi_n]t \end{aligned} \tag{3.4c}$$

$$\Gamma_n = \gamma_n + \lambda_n x - 2\lambda_n\mu_n y - 4\lambda_n(\lambda_n^2 - 3\mu_n^2)t \tag{3.4d}$$

---

[ii] Some entries of the matrix here are complex, however the matrix is self-adjoint, and hence has a real determinant

*2. Then $u(x,y,t)$ is a solution of the KPII equation if the matrix $\mathcal{K}$ has the following entries*

$$K_{nn} = -\Upsilon_n + \frac{\sinh 2\Gamma_n}{2\lambda_n} \tag{3.5a}$$

$$\begin{aligned} K_{nk} &= \frac{(\lambda_n - \lambda_k)\sinh(\Gamma_n - \Gamma_k)}{(\mu_n - \mu_k)^2 - (\lambda_n - \lambda_k)^2} - \frac{(\lambda_n + \lambda_k)\sinh(\Gamma_n + \Gamma_k)}{(\mu_n - \mu_k)^2 - (\lambda_n + \lambda_k)^2} \\ &\quad + \frac{(\mu_n - \mu_k)\cosh(\Gamma_n + \Gamma_k)}{(\mu_n - \mu_k)^2 - (\lambda_n + \lambda_k)^2} + \frac{(\mu_n - \mu_k)\cosh(\Gamma_n - \Gamma_k)}{(\mu_n - \mu_k)^2 - (\lambda_n - \lambda_k)^2}, \\ &\qquad n \neq k \end{aligned} \tag{3.5b}$$

$$\begin{aligned} \Upsilon_n &= \rho_n + x\cosh\chi_n - 2[\lambda_n \sinh\chi_n + \mu_n\cosh\chi_n]y \\ &\quad - 12[\lambda_n^2\cosh\chi_n + \mu_n^2\cosh\chi_n + 2\lambda_n\mu_n\sinh\chi_n]t \end{aligned} \tag{3.5c}$$

$$\Gamma_n = \gamma_n + \lambda_n x - 2\lambda_n\mu_n y - 4\lambda_n(\lambda_n^2 + 3\mu_n^2)t \tag{3.5d}$$

*where $\lambda_n$'s, $\mu_n$'s, $\chi_n$'s, $\gamma_n$'s, $\rho_n$'s are constants, and $n = 1, 2, \cdots, N$.*

*Proof.* We give the proof for the case $\alpha = 1$. We start with the $N$-soliton wall solution in the form

$$u(x,y,t) = 2\frac{\partial^2}{\partial x^2}\ln\det\mathcal{B} \tag{3.6a}$$

where

$$\mathcal{B}_{mn} = \delta_{mn} + \frac{c_n}{p_n + q_m} e^{(p_n+q_m)x + (q_n^2 - p_n^2)y - 4(p_n^3 + q_n^3)t}, \quad m, n = 1, 2, \cdots, 2N. \tag{3.6b}$$

$$\delta_{mn} = \begin{cases} 1 & \text{if} \quad m = n \\ 0 & \text{if} \quad m \neq n \end{cases}$$

and $p_n, q_n, c_n > 0$ are arbitrary constants.

Noticing that both $m$ and $n$ go from 1 to $2N$, we choose

$$\begin{aligned} p_{2k-1} &= -\lambda_k + \mu_k + \varepsilon e^{-\chi_k}, & p_{2k} &= \lambda_k + \mu_k + \varepsilon e^{\chi_k} \\ q_{2k-1} &= -\lambda_k - \mu_k + \varepsilon e^{\chi_k}, & q_{2k} &= \lambda_k - \mu_k + \varepsilon e^{-\chi_k} \\ c_{2k-1} &= 2\varepsilon e^{-2\gamma_k + 2\rho_k \varepsilon}, & c_{2k} &= 2\varepsilon e^{2\gamma_k + 2\rho_k \varepsilon} \end{aligned} \tag{3.7}$$

$$\lambda_k, \mu_k, \chi_k, \gamma_k, \rho_k \in \Re, \; k = 1, 2, \cdots, N$$

$$\varepsilon \text{ is a perturbation parameter.}$$

The substitution of (3.7) into (3.6) gives the transformation

$$u(x, y, t) = 2 \frac{\partial^2}{\partial x^2} \ln \det \mathcal{B}^\varepsilon \tag{3.8}$$

where

$$\mathcal{B}^\varepsilon = \begin{pmatrix} \mathcal{B}^\varepsilon_{11} & \mathcal{B}^\varepsilon_{12} & \cdots & \mathcal{B}^\varepsilon_{1N} \\ \mathcal{B}^\varepsilon_{21} & \mathcal{B}^\varepsilon_{22} & \cdots & \mathcal{B}^\varepsilon_{2N} \\ \vdots & \vdots & \vdots & \vdots \\ \mathcal{B}^\varepsilon_{N1} & \mathcal{B}^\varepsilon_{N2} & \cdots & \mathcal{B}^\varepsilon_{NN} \end{pmatrix} \tag{3.9}$$

with $2 \times 2$ block entries

$$\mathcal{B}^\varepsilon_{mn} = \begin{pmatrix} \mathcal{B}^\varepsilon_{mn,11} & \mathcal{B}^\varepsilon_{mn,12} \\ \mathcal{B}^\varepsilon_{mn,21} & \mathcal{B}^\varepsilon_{mn,22} \end{pmatrix} \tag{3.10}$$

$$\mathcal{B}^{\varepsilon}_{mn,11} = \delta_{mn} + \frac{c_{2n-1}}{p_{2n-1}+q_{2m-1}} e^{(p_{2n-1}+q_{2m-1})x+(q^2_{2n-1}-p^2_{2n-1})y-4(p^3_{2n-1}+q^3_{2n-1})t}$$

$$\mathcal{B}^{\varepsilon}_{mn,12} = \frac{c_{2n}}{p_{2n}+q_{2m-1}} e^{(p_{2n}+q_{2m})x+(q^2_{2n}-p^2_{2n})y-4(p^3_{2n}+q^3_{2n})t}$$

$$\mathcal{B}^{\varepsilon}_{mn,21} = \frac{c_{2n-1}}{p_{2n-1}+q_{2m}} e^{(p_{2n-1}+q_{2m-1})x+(q^2_{2n-1}-p^2_{2n-1})y-4(p^3_{2n-1}+q^3_{2n-1})t}$$

$$\mathcal{B}^{\varepsilon}_{mn,22} = \delta_{mn} + \frac{c_{2n}}{p_{2n}+q_{2m}} e^{(p_{2n}+q_{2m})x+(q^2_{2n}-p^2_{2n})y-4(p^3_{2n}+q^3_{2n})t}$$

$\delta_{mn}$ are the regular Kronecker symbols.

Then

$$\det \mathcal{B}^{\varepsilon} = \sum_{\sigma \in S_{2N}} \operatorname{sgn}(\sigma) \prod_{i=1}^{N} \mathcal{D}^{\varepsilon}_{i\sigma_i} \tag{3.11}$$

where $S_{2N}$ is the group of permutations of $\{1, 2, \cdots, 2N\}$, and $\sigma_i = \{k_1, k_2, \cdots, k_{2N}\} \in S_{2N}$. $\mathcal{D}^{\varepsilon}_{i\sigma_i}$ are the $2 \times 2$ matrices obtained by taking the elements of $\mathcal{B}^{\varepsilon}$ at the intersection of the $(2i-1)-th$ and $(2i)-th$ rows, and the $k_{2i-1}-th$ and $k_{2i}-th$ columns, with $k_{2i-1} < k_{2i}$. These $2 \times 2$ matrices have the following determinants as $\varepsilon \to 0$ :

1. if $k_{2i-1} = 2i-1$ and $k_{2i} = 2i$, then

$$\det \mathcal{D}^{\varepsilon}_{2i-1\ 2i\ k_{2i-1}\ k_{2i}} = \det \mathcal{B}^{\varepsilon}_{ii} = 4\varepsilon \left[ -\Upsilon_i + \frac{\sinh 2\Gamma_i}{2\lambda_i} \right] + O(\varepsilon^2) \tag{3.12a}$$

2. if $k_{2i-1} = 2i - 1$ and $k_{2i} \neq 2i$, then

$$\det \mathcal{D}^{\varepsilon}_{2i-1\ 2i\ k_{2i-1}k_{2i}} = \tag{3.12b}$$
$$- 2\varepsilon \left[ \frac{\cosh(\Gamma_{ki_1} - \Gamma_{ki_2})}{(\mu_{ki_1} - \mu_{ki_2}) - (\lambda_{ki_1} - \lambda_{ki_2})} + \frac{\sinh(\Gamma_{ki_1} - \Gamma_{ki_2})}{(\mu_{ki_1} - \mu_{ki_2}) - (\lambda_{ki_1} - \lambda_{ki_2})} \right.$$
$$\left. + \frac{\cosh(\Gamma_{ki_1} + \Gamma_{ki_2})}{(\mu_{ki_1} - \mu_{ki_2}) - (\lambda_{ki_1} + \lambda_{ki_2})} + \frac{\sinh(\Gamma_{ki_1} + \Gamma_{ki_2})}{(\mu_{ki_1} - \mu_{ki_2}) - (\lambda_{ki_1} + \lambda_{ki_2})} \right] + O(\varepsilon^2)$$

3. if $k_{2i-1} \neq 2i - 1$ and $k_{2i} = 2i$, then

$$\det \mathcal{D}^{\varepsilon}_{2i-1\ 2i\ k_{2i-1}k_{2i}} = \tag{3.12c}$$
$$- 2\varepsilon \left[ \frac{\cosh(\Gamma_{ki_1} - \Gamma_{ki_2})}{(\mu_{ki_1} - \mu_{ki_2}) + (\lambda_{ki_1} - \lambda_{ki_2})} - \frac{\sinh(\Gamma_{ki_1} - \Gamma_{ki_2})}{(\mu_{ki_1} - \mu_{ki_2}) + (\lambda_{ki_1} - \lambda_{ki_2})} \right.$$
$$\left. + \frac{\cosh(\Gamma_{ki_1} + \Gamma_{ki_2})}{(\mu_{ki_1} - \mu_{ki_2}) + (\lambda_{ki_1} + \lambda_{ki_2})} - \frac{\sinh(\Gamma_{ki_1} + \Gamma_{ki_2})}{(\mu_{ki_1} - \mu_{ki_2}) + (\lambda_{ki_1} + \lambda_{ki_2})} \right] + O(\varepsilon^2)$$

4. if $k_{2i-1} \neq 2i - 1$ and $k_{2i} \neq 2i$, then

$$\det \mathcal{D}^{\varepsilon}_{2i-1\ 2i\ k_{2i-1}k_{2i}} = O(\varepsilon^2) \tag{3.12d}$$

As $\varepsilon \to 0$ we obtain that $u(x, y, t)$ as defined by equation (3.5) satisfies the KPII equation.

For the change of variables $y = \alpha^{-1} y^*$, $\mu_n = \alpha \mu_n^*$ and $\chi_n = \alpha \chi_n^*$, we obtain as proof that $u(x, y, t)$ as defined by equation (3.4) satisfies the KPI equation. □

How do we understand the formulas in **Theorem 1**? For $N = 1$, we obtain one such explicit solution (soliton), for $N = 2$, we obtain the interaction of two such explicit solutions (interaction between two solitons), and so on. The formula given in **Theorem 1** describes the nonlinear interaction of $N$ solutions (interaction between $N$ solitons).

In this thesis, we are only interested in describing the nature of one such solution ($N = 1$), and the simulations for two such solutions ($N = 2$). The general study of the nonlinear interactions of these singular solutions is quite involved and will be a good study for future work.

## 3.2 Singular Solutions

In this section, we consider the simplest form of the solutions of equations (3.4) and (3.5). For the KPI equation ($\alpha = i$), we have the singular solution of (3.4) as

$$u(x, y, t) = \frac{8\lambda_1^3 \sinh 2\Gamma_1}{2\Upsilon_1 + \lambda_1 \sinh 2\Gamma_1} - 8\left[\frac{\cos\chi_1 + \lambda_1^2 \cosh 2\Gamma_1}{2\Upsilon_1 + \lambda_1 \sinh 2\Gamma_1}\right]^2 \tag{3.13a}$$

$$\begin{aligned}\Upsilon_1 \quad = \quad & \rho_1 + x\cos\chi_1 - 2[\lambda_1 \sin\chi_1 + \mu_1 \cos\chi_1]y \\ & - 12[\lambda_1^2 \cos\chi_1 - \mu_1^2 \cos\chi_1 - 2\lambda_1\mu_1 \sin\chi_1]t\end{aligned} \tag{3.13b}$$

$$\Gamma_1 = \gamma_1 + \lambda_1 x - 2\lambda_1\mu_1 y - 4\lambda_1(\lambda_1^2 - 3\mu_1^2)t \tag{3.13c}$$

Each singular solution is characterized by the essential parameters (spectral pair) $\lambda_1$ and $\mu_1$.

The solution (3.13) is a singular solution and due to the fact that the range of the sinh function is $(-\infty, \infty)$, then for any spatial domain $(x, y)$, we will encounter singularities in time. We can isolate small domains where we do not have singularities for limited amounts of time, but this is not the purpose of this work. We are interested to see how these singularities behave within the system and what role they play in the formation of rogue waves. Is there any “rule” in the chaos they are usually associated with?

From the simulations of the nonlinear interaction of two of such singular solutions it seems there is, but the mathematical "truth" is deeply hidden in the complex structure of their interaction.

In this thesis we just observe through the time simulations that we make how the singular solutions that are notorious to bring chaos into a system can actually create a certain order through their nonlinear interaction.

The wave profile of (3.13) moves with a velocity $\mathbf{v} = (v_x, v_y)$, where $v_x$ and $v_y$ are the velocities in the $x-$ and $y-$directions respectively.

We determine the velocity components from the linear system

$$v_x - 2[\lambda_1 \tan\chi_1 + \mu_1]v_y = 12[\lambda_1^2 - \mu_1^2 - 2\lambda_1\mu_1 \tan\chi_1] \tag{3.14a}$$

$$v_x - 2\mu_1 v_y = 4(\lambda_1^2 - 3\mu_1^2) \tag{3.14b}$$

If the determinant of system (3.14) is nonzero, the system has a unique solution

$$v_x = 4(\lambda_1^2 + 3\mu_1^2) - \frac{8\lambda_1\mu_1}{\tan\chi_1} \tag{3.15a}$$

$$v_y = 12\mu_1 - \frac{4\lambda_1}{\tan\chi_1} \tag{3.15b}$$

The velocity vector $\mathbf{v}$ is never zero. The velocity $\mathbf{v} = (v_x, v_y)$ is the velocity of the motion of the wave profile, and should not be confused with $\mathbf{u}'$, which is the velocity of the fluid motion.

The solution (3.13) is singular and approaches $-\infty$. Where these singularities occur, the KP model fails, however, we should not be deterred by this, it is just like Coulomb's law in electrostatics. Away from these singularities, the model is valid and gives good solutions. For the model to be physically correct, we need to remove the singularities. However, there is no particular way of regulating these singularities.

We choose the ad-hoc regularization

$$U = e^u - 1 \tag{3.16}$$

due to its properties

$$\begin{aligned} &U = 0, \text{ if } u = 0 \\ &U \to -1, \text{ as } u \to -\infty \end{aligned} \tag{3.17}$$

Enormous energy from these singularities gives rise to the rogue waves. The case $N = 2$ is meant to be at an observational level. We will observe in Section 3.3, a very interesting situation which leads to the idea that the Kadomtsev-Petviashvili model can be a good start to the understanding of rogue waves.

Here, we see the graphs of singular waves for both the KPI and KPII equations.

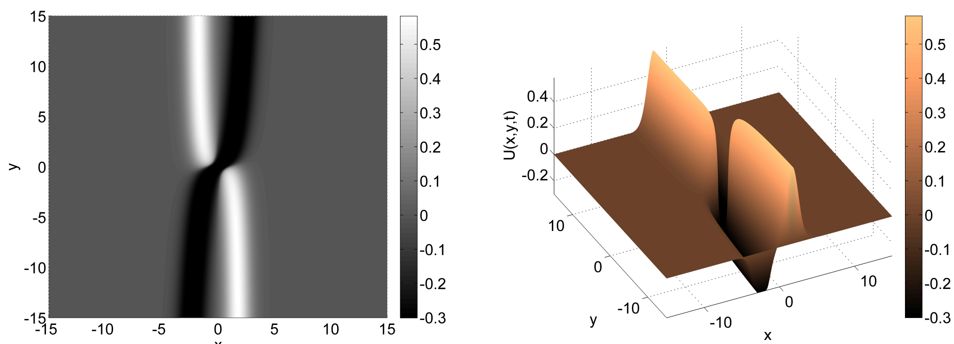


(a) Projection onto $xy$-plane

(b) 3D plot

Figure 3.1: Singular Wave of the KPI equation with $\chi_1 = 0.9$, $\lambda_1 = 1.2$, $\mu_1 = 0.01$, $\gamma_1 = 0$, $\rho_1 = 0$, at $t = 0$.

Figure 3.1 shows the graph of $U$[iii], where $u$ is as given by equation (3.13). The fluid moves to the left for $U < 0$, shown in regions with dark shadings in Figure 3.1; the fluid moves to the right for $U > 0$, shown in regions with light shadings in Figure 3.1. When the fluid moving to the left collides with the fluid moving to the right, we obtain a point of "crossing" of dark and light shades. The velocity of motion of the fluid at this point is as given in equation (3.15). Here are other graphs of equation (3.13).

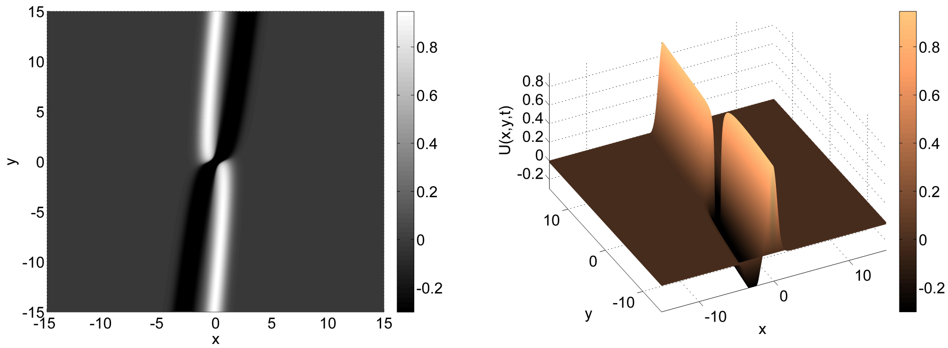


(a) Projection onto $xy$-plane (b) 3D plot

Figure 3.2: Singular Wave of the KPI equation with $\chi_1 = 0.5$, $\lambda_1 = 2$, $\mu_1 = 0.05$, $\gamma_1 = 0$, $\rho_1 = 0$, at $t = 0$.

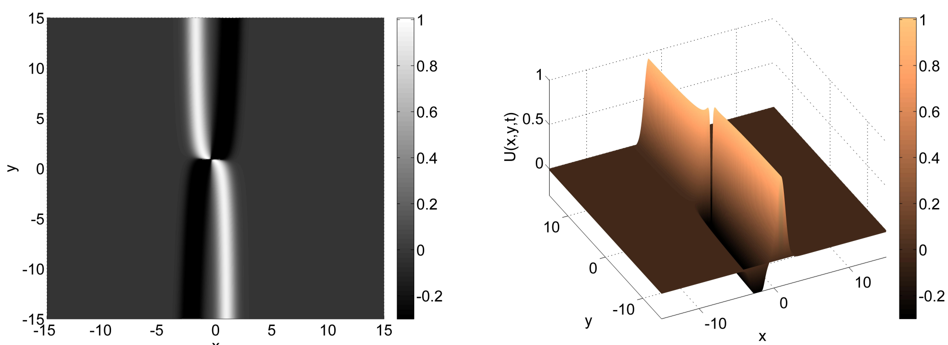


(a) Projection onto $xy$-plane (b) 3D plot

Figure 3.3: Singular Wave of the KPI equation with $\chi_1 = 2$, $\lambda_1 = 1.95$, $\mu_1 = 0.006$, $\gamma_1 = 0.8$, $\rho_1 = 3$, at $t = 0$.

iii $U = e^u - 1$

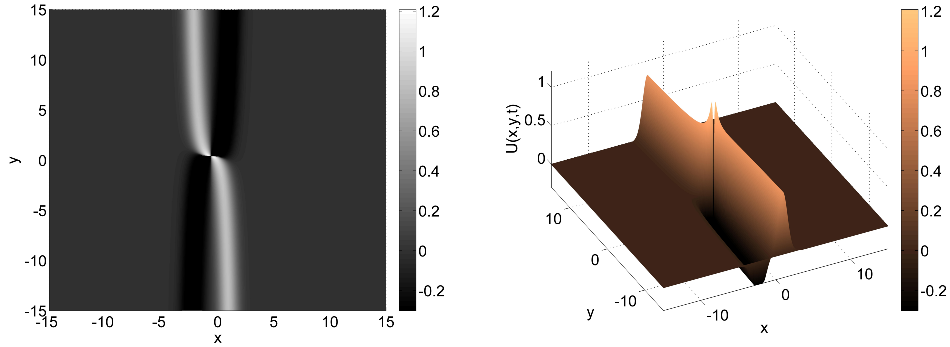


(a) Projection onto $xy$-plane

(b) 3D plot

Figure 3.4: Singular Wave of the KPI equation with $\chi_1 = 2.5$, $\lambda_1 = 1.65$, $\mu_1 = 0.01$, $\gamma_1 = 1$, $\rho_1 = 0.3$, at $t = 0$.

For the KPII equation ($\alpha = 1$), we have the single wave solution of (3.5) as

$$u(x, y, t) = -\frac{8\lambda_1^3 \sinh 2\Gamma_1}{2\Upsilon_1 - \lambda_1 \sinh 2\Gamma_1} - 8\left[\frac{\cosh \chi_1 - \lambda_1^2 \cosh 2\Gamma_1}{2\Upsilon_1 - \lambda_1 \sinh 2\Gamma_1}\right]^2 \qquad (3.18a)$$

$$\begin{aligned} \Upsilon_1 \;&=\; \rho_1 + x \cosh \chi_1 - 2[\lambda_1 \sinh \chi_1 + \mu_1 \cosh \chi_1]y \qquad (3.18b) \\ &\quad - 12[\lambda_1^2 \cosh \chi_1 + \mu_1^2 \cosh \chi_1 + 2\lambda_1\mu_1 \sinh \chi_1]t \end{aligned}$$

$$\Gamma_1 = \gamma_1 + \lambda_1 x - 2\lambda_1\mu_1 y - 4\lambda_1(\lambda_1^2 + 3\mu_1^2)t \qquad (3.18c)$$

The wave profile of (3.18) also moves with a velocity $\mathbf{v} = (v_x, v_y)$, where $v_x$ and $v_y$ are the same as defined for the wave profile of (3.13). We determine these components from the linear system

$$v_x - 2[\lambda_1 \tanh \chi_1 + \mu_1]v_y = 12[\lambda_1^2 + \mu_1^2 + 2\lambda_1\mu_1 \tanh \chi_1] \qquad (3.19a)$$

$$v_x - 2\mu_1 v_y = 4(\lambda_1^2 + 3\mu_1^2) \qquad (3.19b)$$

If the determinant of this system in nonzero, we find the unique velocities as

$$v_x = 4(\lambda_1^2 - 3\mu_1^2) - \frac{8\lambda_1\mu_1}{\tanh\chi_1} \tag{3.20a}$$

$$v_y = -12\mu_1 - \frac{4\lambda_1}{\tanh\chi_1} \tag{3.20b}$$

The explanations that applied to the wave profile (3.13) are the similar for the wave profile (3.18) and we will use the same regularization as (3.13).

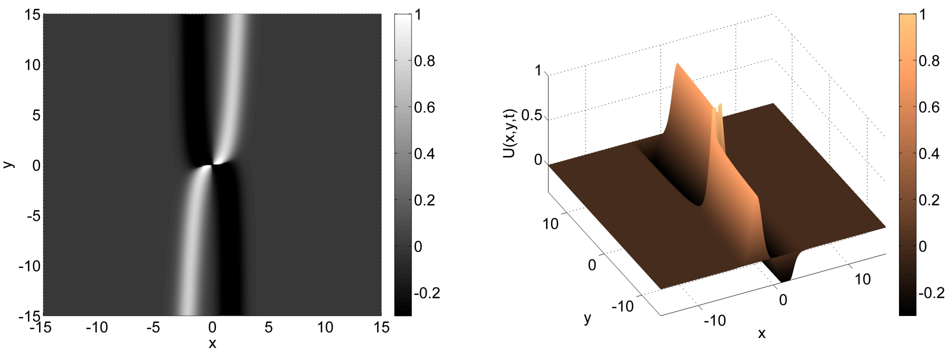


(a) Projection onto $xy$-plane (b) 3D plot

Figure 3.5: Singular Wave of the KPII equation with $\chi_1 = 1$, $\lambda_1 = 1.5$, $\mu_1 = 0.01$, $\gamma_1 = 0$, $\rho_1 = 0$, at $t = 0$.

Figure 3.5 shows the graph of $U^{\text{iv}}$, where $u$ is as given by equation (3.18). The fluid moves to the left for $U < 0$, shown in regions with dark shadings in 3.5; the fluid moves to the right for $U > 0$, shown in regions with light shadings in 3.5. When the fluid moving to the left collides with the fluid moving to the right, we obtain a point of "crossing" of dark and light shades. The velocity of motion of the fluid at this point is as given in equation (3.20).

[iv] $U = e^u - 1$

Here are other graphs of equation (3.18).

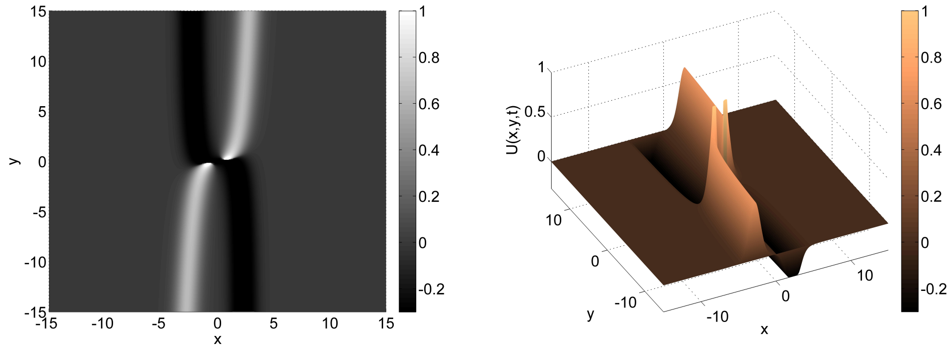


(a) Projection onto $xy$-plane (b) 3D plot

Figure 3.6: Singular Wave of the KPII equation with $\chi_1 = 2$, $\lambda_1 = 1.3$, $\mu_1 = 0.009$, $\gamma_1 = 0$, $\rho_1 = 0$, at $t = 0$.

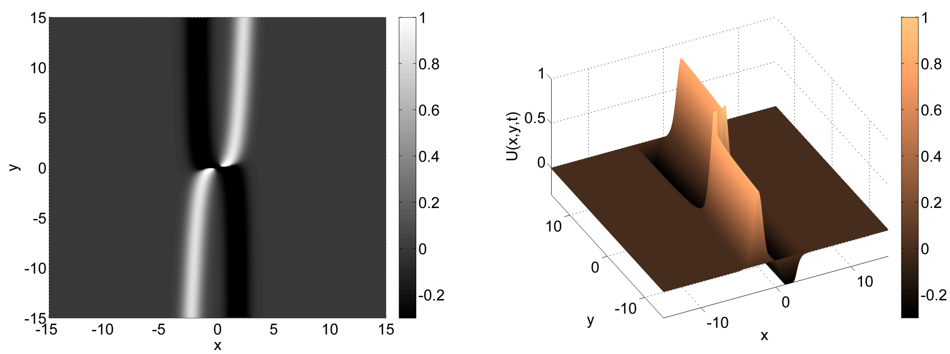


(a) Projection onto $xy$-plane (b) 3D plot

Figure 3.7: Singular Wave of the KPII equation with $\chi_1 = 1.9$, $\lambda_1 = 1.7$, $\mu_1 = 0.01$, $\gamma_1 = 0$, $\rho_1 = 0.2$, at $t = 0$.

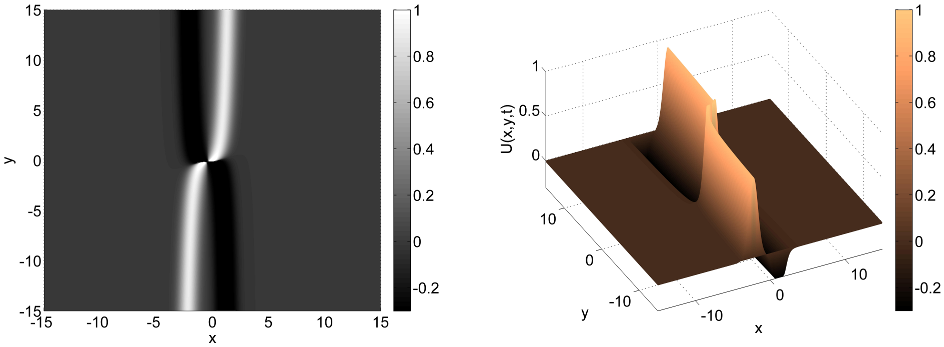


(a) Projection onto $xy$-plane (b) 3D plot

Figure 3.8: Singular Wave of the KPII equation with $\chi_1 = 1.1$, $\lambda_1 = 1.85$, $\mu_1 = 0.002$, $\gamma_1 = 0.8$, $\rho_1 = 0$, at $t = 0$.

Each graph in Figures 3.5, 3.6, 3.7 and 3.8 have been cut at the top, to improve visualization.

The singularities break the solution into two simple-connected waves, each of which is a solution of the KP equation. Each wave moves like a soliton, just like the waves observed in oceans. This can be observed from the Figures shown below. Figure 3.9 shows the graph of $U$, where $u$ is

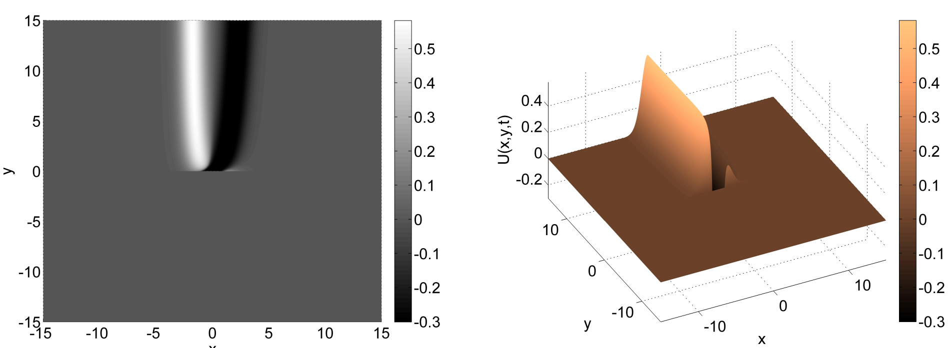


(a) Projection onto $xy$-plane (b) 3D plot

Figure 3.9: Simple-Connected Wave of the KPI equation with $\chi_1 = 0.9$, $\lambda_1 = 1.2$, $\mu_1 = 0.01$, $\gamma_1 = 0$, $\rho_1 = 0$, at $t = 0$.

as given by equation (3.13) and it is an example of the simple-connected waves. This graph is similar to what we observe in Figure 3.10, for $u$

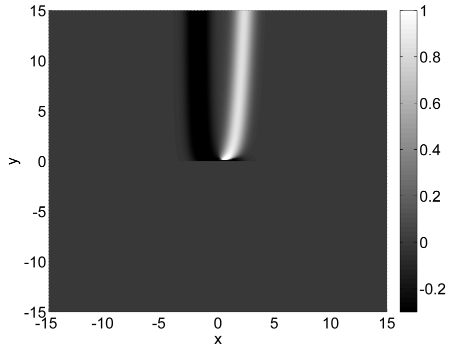


(a) Projection onto $xy$-plane

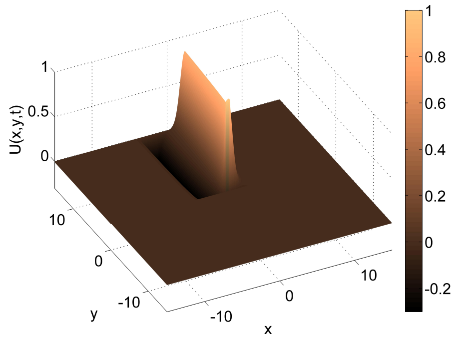


(b) 3D plot

Figure 3.10: Simple-Connected Wave of the KPII equation with $\chi_1 = 1.9$, $\lambda_1 = 1.7$, $\mu_1 = 0.01$, $\gamma_1 = 0$, $\rho_1 = 0.2$, at $t = 0$.

Figure 3.11: A rogue wave that compares to Figures 3.9 and 3.10

as given by equation (3.18) and can be compared to the picture in Figure 3.11 (http://www.popsci.com/science/article/2009-11/econophysicists-rogue-waves-could-account-volatility-financial-markets).

Figure 3.11 shows how the water wave collects at it's highest point of elevation. We observed similarities in the depression and elevation of Figures 3.9 and 3.10, compared with the picture in Figure 3.11. This could be as a result of wind blowing over a calm water surface, therefore generating ripples which are affected by gravity and surface tension. Over a period of time, energy builds up between high and low frequencies. Some energy is lost as a result of breaking, and the rest of the energy is transfered by nonlinear effects to the lower frequencies causing a sudden change in peaks.

## 3.3 Interaction of Singular Solutions[v]

In this section, we will show how the Kadomtsev-Petviashvili equation predicts the occurrence of rogue waves. Some aspects of the waves we will study will be considered non-physical due to how thin they are. The KP equation does not take into account wave-overturning, this therefore does not make the KP equation a good model for traveling waves.

In this section, we consider the case $N = 2$ for both equations (3.4) and (3.5). This will give us the interaction of two singular waves. Below, we give the time evolution of the singular waves of Figures 3.1 and 3.2. Since the matrix of the solutions (3.4) and (3.5) are symmetric, we will only move forward in time, that is from $t = 0$ to $t = 0.2$. Moving backwards in time gives us the same solution but in the opposite direction. Here are the graphs;

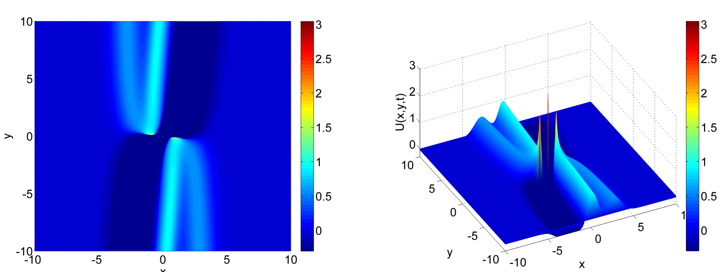


(a) Projection onto $xy$-plane (b) 3D plot

Figure 3.12: Interaction of two singular waves with $\chi_1 = 0.9$, $\chi_2 = 0.5$, $\lambda_1 = 1.2$, $\lambda_2 = 2$, $\mu_1 = 0.01$, $\mu_2 = 0.05$, $\gamma_1 = \gamma_2 = 0$, $\rho_1 = \rho_2 = 0$, at $t = 0$.

[v] As suggested by Dr. Kovalyov (supervisor), we studied interaction of singular solutions

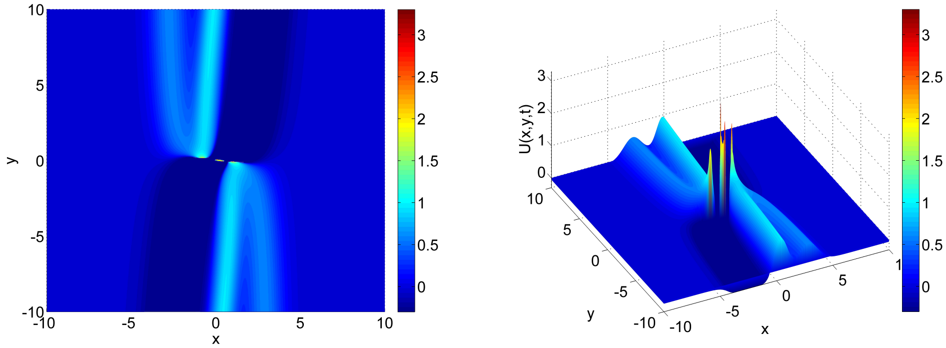


(a) Projection onto $xy$-plane (b) 3D plot

Figure 3.13: Interaction of two singular waves with $\chi_1 = 0.9$, $\chi_2 = 0.5$, $\lambda_1 = 1.2$, $\lambda_2 = 2$, $\mu_1 = 0.01$, $\mu_2 = 0.05$, $\gamma_1 = \gamma_2 = 0$, $\rho_1 = \rho_2 = 0$, at $t = 0.01$.

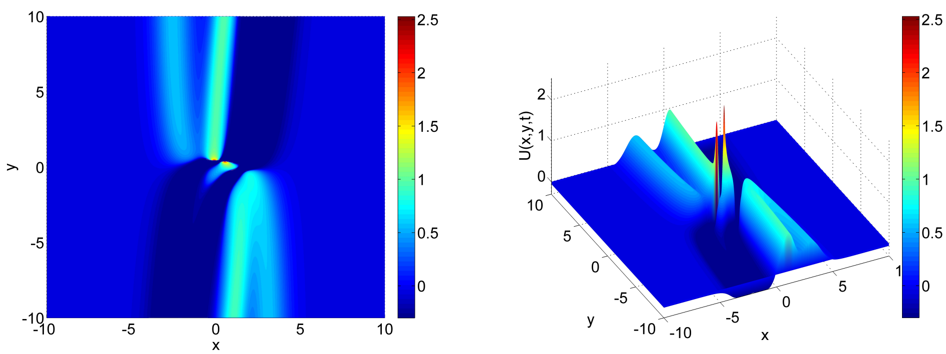


(a) Projection onto $xy$-plane (b) 3D plot

Figure 3.14: Interaction of two singular waves with $\chi_1 = 0.9$, $\chi_2 = 0.5$, $\lambda_1 = 1.2$, $\lambda_2 = 2$, $\mu_1 = 0.01$, $\mu_2 = 0.05$, $\gamma_1 = \gamma_2 = 0$, $\rho_1 = \rho_2 = 0$, at $t = 0.05$.

Figures 3.12 to 3.17 show the time evolution of the interaction of $U$, where $u$ is as given by equation (3.4). We observe that the amplitude of the wave was high at time $t = 0$, and started decreasing after. We however see that at times $t = 0.01$ and $t = 0.1$, the amplitudes (peaks) are higher than at time $t = 0$. We consider the waves in this situation unphysical, since they are not strong enough to stand alone, and will therefore collapse. Taking a closer look at the views will make this clearer. This time evolution shows that the life span of the wave formed from the interaction of the two singular waves of Figures 3.1 and 3.2 is very short.

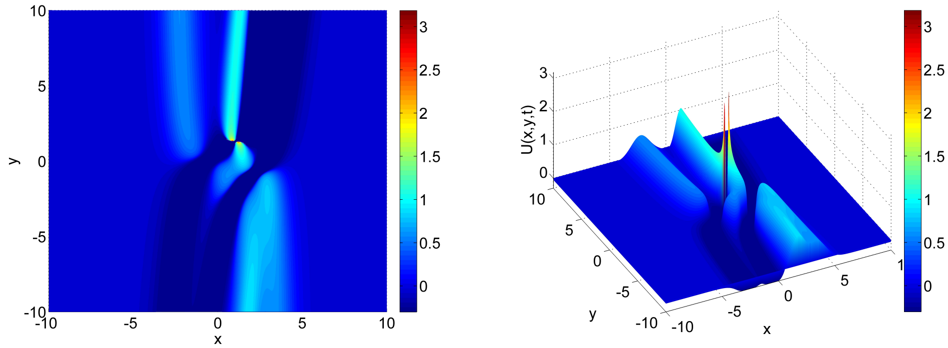


(a) Projection onto $xy$-plane (b) 3D plot

Figure 3.15: Interaction of two singular waves with $\chi_1 = 0.9$, $\chi_2 = 0.5$, $\lambda_1 = 1.2$, $\lambda_2 = 2$, $\mu_1 = 0.01$, $\mu_2 = 0.05$, $\gamma_1 = \gamma_2 = 0$, $\rho_1 = \rho_2 = 0$, at $t = 0.1$.

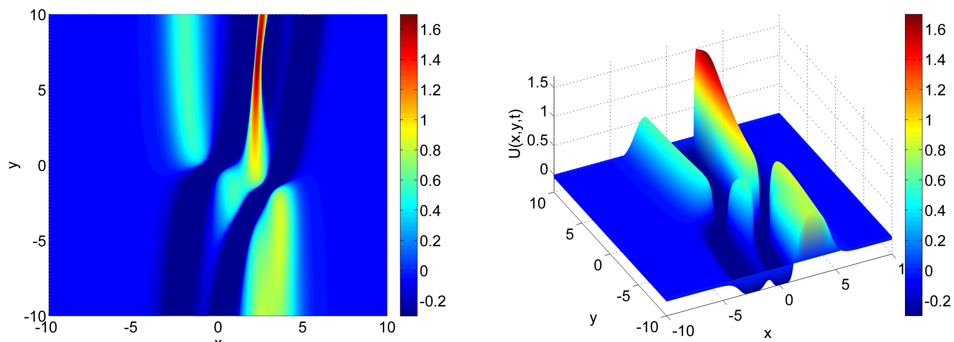


(a) Projection onto $xy$-plane (b) 3D plot

Figure 3.16: Interaction of two singular waves with $\chi_1 = 0.9$, $\chi_2 = 0.5$, $\lambda_1 = 1.2$, $\lambda_2 = 2$, $\mu_1 = 0.01$, $\mu_2 = 0.05$, $\gamma_1 = \gamma_2 = 0$, $\rho_1 = \rho_2 = 0$, at $t = 0.15$.

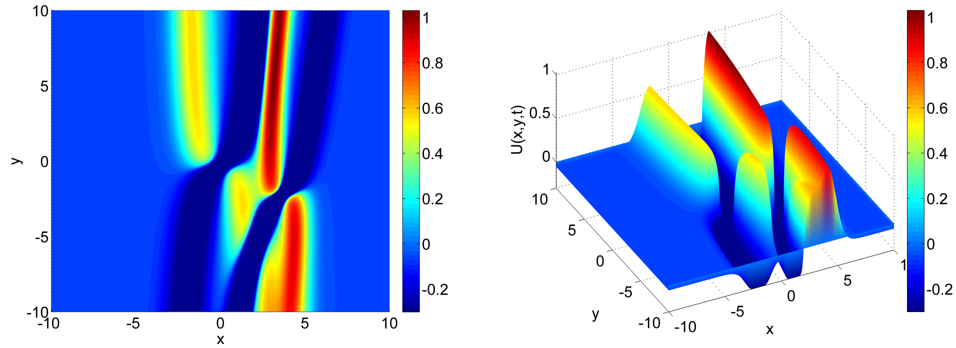


(a) Projection onto $xy$-plane (b) 3D plot

Figure 3.17: Interaction of two singular waves with $\chi_1 = 0.9$, $\chi_2 = 0.5$, $\lambda_1 = 1.2$, $\lambda_2 = 2$, $\mu_1 = 0.01$, $\mu_2 = 0.05$, $\gamma_1 = \gamma_2 = 0$, $\rho_1 = \rho_2 = 0$, at $t = 0.2$.

We will now take a closer look at the amplitudes of the waves occurring at a time before ($t = -0.1$), at $t = 0$, and the time after ($t = 0.1$) in Figures 3.18, 3.19 and 3.20.

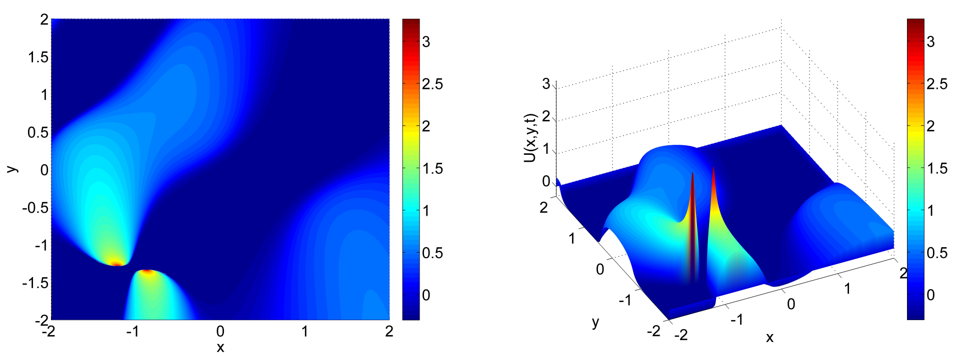


(a) Projection onto $xy$-plane (b) 3D plot

Figure 3.18: Interaction of two singular waves with $\chi_1 = 0.9$, $\chi_2 = 0.5$, $\lambda_1 = 1.2$, $\lambda_2 = 2$, $\mu_1 = 0.01$, $\mu_2 = 0.05$, $\gamma_1 = \gamma_2 = 0$, $\rho_1 = \rho_2 = 0$, at $t = -0.1$.

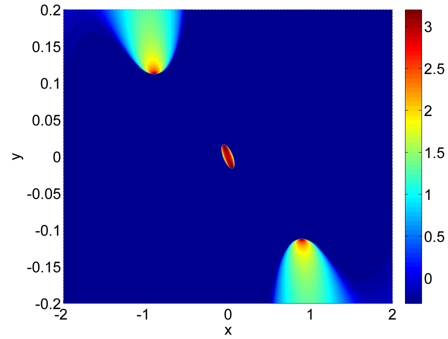


(a) Projection onto $xy$-plane

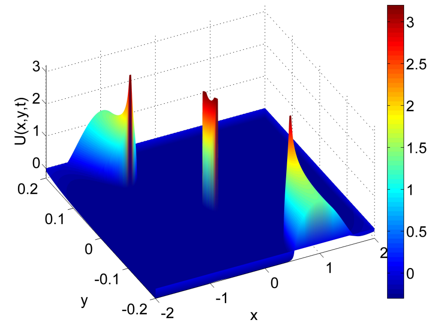


(b) 3D plot

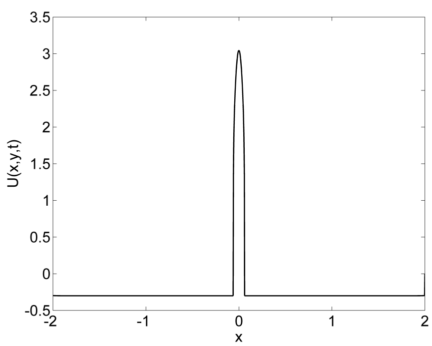


(c) Cross-Section by plane $y = 0$

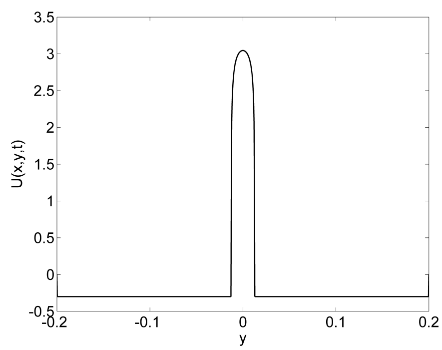


(d) Cross-Section by plane $x = 0$

Figure 3.19: Interaction of two singular waves with $\chi_1 = 0.9$, $\chi_2 = 0.5$, $\lambda_1 = 1.2$, $\lambda_2 = 2$, $\mu_1 = 0.01$, $\mu_2 = 0.05$, $\gamma_1 = \gamma_2 = 0$, $\rho_1 = \rho_2 = 0$, at $t = 0$.

We notice that the waves will have an inelastic collision and observe that energy accumulates to increase the amplitude of a new wave, much larger than the ones creating it. This gives us an idea that the KP model may describe up to a point the evolution of a rogue wave. The more waves would collide with each other's at the same time, the larger the amplitude of the new wave; this is the birth of a rogue wave. As the amplitude grows larger and larger, the KP equation fails at some point when the surface becomes multi-valued and the waves break. The waves of interest to us are Figure 3.19, Figure 3.18 (backwards in time $t = -0.1$) and Figure 3.20 (forward in time $t = 0.1$), they show the wave appearing from nowhere.

The two small peaks in Figure 3.19 are very thin and should be considered unphysical since they are not strong enough to support themselves, and will therefore, collapse.

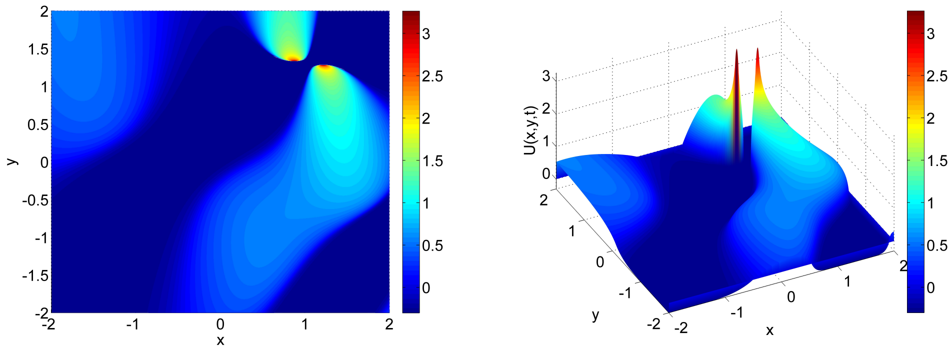


(a) Projection onto $xy$-plane (b) 3D plot

Figure 3.20: Interaction of two singular waves with $\chi_1 = 0.9$, $\chi_2 = 0.5$, $\lambda_1 = 1.2$, $\lambda_2 = 2$, $\mu_1 = 0.01$, $\mu_2 = 0.05$, $\gamma_1 = \gamma_2 = 0$, $\rho_1 = \rho_2 = 0$, at $t = 0.1$.

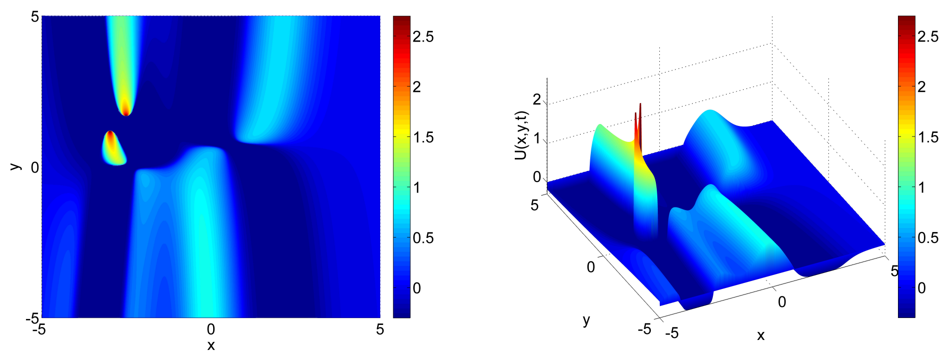


(a) Projection onto $xy$-plane (b) 3D plot

Figure 3.21: Interaction of two singular waves with $\chi_1 = 0.6$, $\chi_2 = 5$, $\lambda_1 = 1.8$, $\lambda_2 = 1.5$, $\mu_1 = 0.007$, $\mu_2 = 0.0005$, $\gamma_1 = \gamma_2 = 0$, $\rho_1 = \rho_2 = 0$, at $t = -0.1$.

Figure 3.21 above, and Figures 3.22 and 3.24 below, show the graph of the time evolution of the solution of equation (3.4). This is an interesting case where the energy accumulates into a single peak as in Figure 3.22. We observe in Figures 3.21 and 3.24 that, the amplitude is smaller than the amplitude in Figure 3.22. We should also take note of the elevations and depressions surrounding the wave. Elevations and depressions are observed whenever a rogue wave occurs.

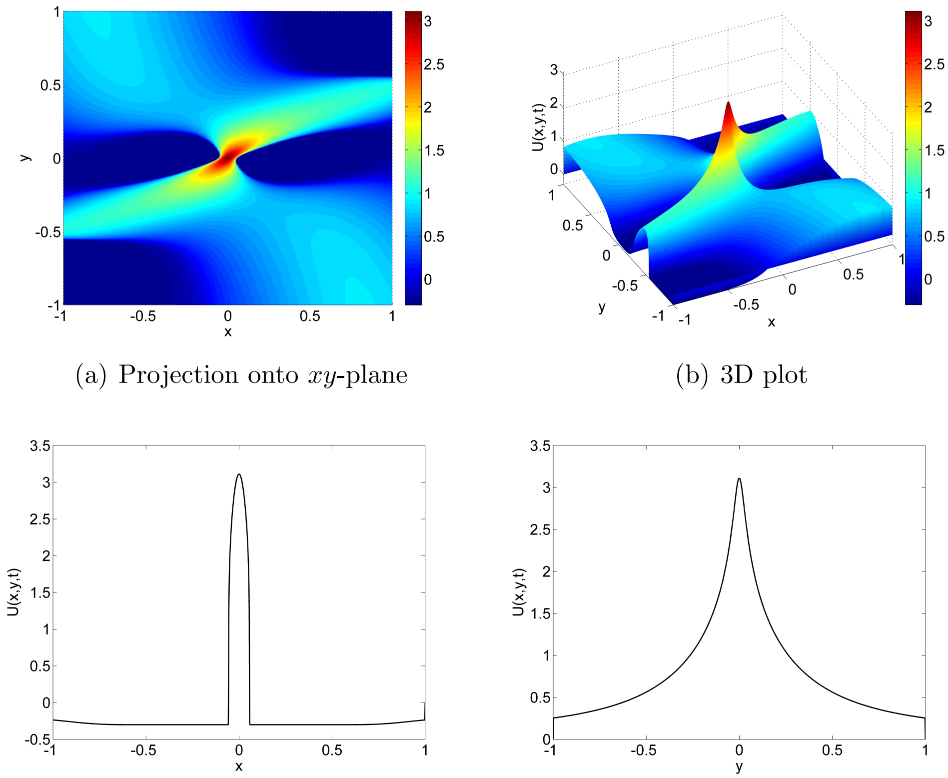


(a) Projection onto $xy$-plane

(b) 3D plot

(c) Cross-Section by plane $y = 0$

(d) Cross-Section by plane $x = 0$

Figure 3.22: Interaction of two singular waves with $\chi_1 = 0.6$, $\chi_2 = 5$, $\lambda_1 = 1.8$, $\lambda_2 = 1.5$, $\mu_1 = 0.007$, $\mu_2 = 0.0005$, $\gamma_1 = \gamma_2 = 0$, $\rho_1 = \rho_2 = 0$, at $t = 0$.

Figure 3.23 below (http://www.armageddononline.org/Rogue-Waves-and-Freak-Waves.html) shows an example of a rogue wave, that is similar to the graph in Figure 3.22. Figure 3.22 may be similar to Figure 3.23 when we compare how the wave builds up, and also the elevations and depressions of the surrounding water.

Figure 3.23: An example of a rogue wave similar to Figure 3.22

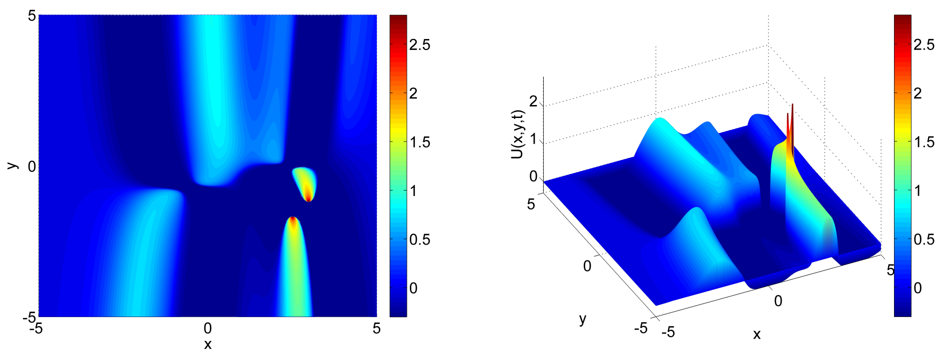


(a) Projection onto $xy$-plane

(b) 3D plot

Figure 3.24: Interaction of two singular waves with $\chi_1 = 0.6$, $\chi_2 = 5$, $\lambda_1 = 1.8$, $\lambda_2 = 1.5$, $\mu_1 = 0.007$, $\mu_2 = 0.0005$, $\gamma_1 = \gamma_2 = 0$, $\rho_1 = \rho_2 = 0$, at $t = 0.1$.

Figures 3.25, 3.26 and 3.27 below show the time evolution of the interaction of the singular waves of Figures 3.3 and 3.4. We notice that the collision of the two different waves cause an increase in the amplitude of the new wave created as a result of the interaction. Here we observe that there are three different peaks, however, two of them are small in such a way that they do not have enough energy to support themselves. This could be due to the limitations of the KP equation as a model.

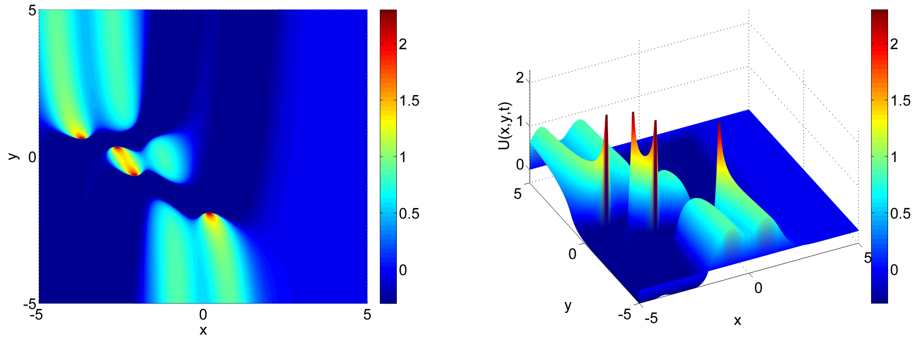


(a) Projection onto $xy$-plane (b) 3D plot

Figure 3.25: Interaction of two singular waves with $\chi_1 = 2$, $\chi_2 = 2.5$, $\lambda_1 = 1.95$, $\lambda_2 = 1.65$, $\mu_1 = 0.006$, $\mu_2 = 0.01$, $\gamma_1 = 0.8$, $\gamma_2 = 1$, $\rho_1 = 3$, $\rho_2 = 0.3$, at $t = -0.1$.

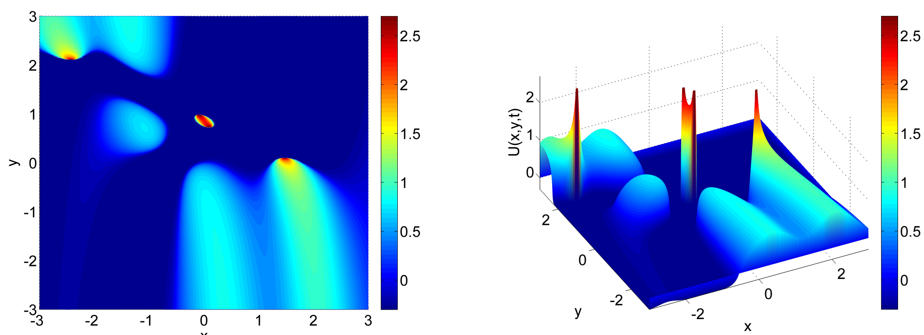


(a) Projection onto $xy$-plane (b) 3D plot

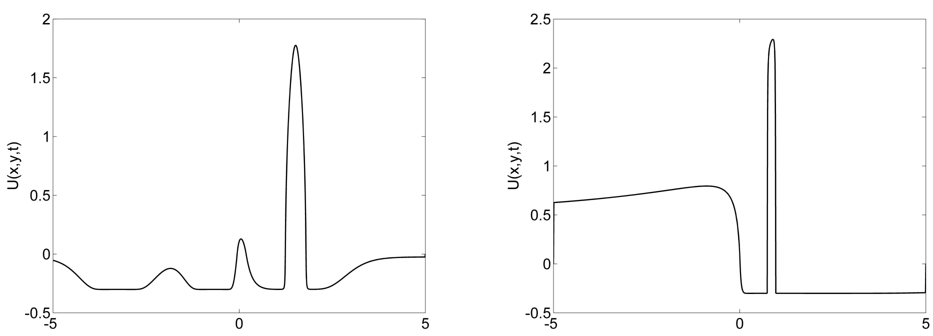


(c) Cross-Section by plane $y = 0$ (d) Cross-Section by plane $x = 0$

Figure 3.26: Interaction of two singular waves with $\chi_1 = 2$, $\chi_2 = 2.5$, $\lambda_1 = 1.95$, $\lambda_2 = 1.65$, $\mu_1 = 0.006$, $\mu_2 = 0.01$, $\gamma_1 = 0.8$, $\gamma_2 = 1$, $\rho_1 = 3$, $\rho_2 = 0.3$, at $t = 0$.

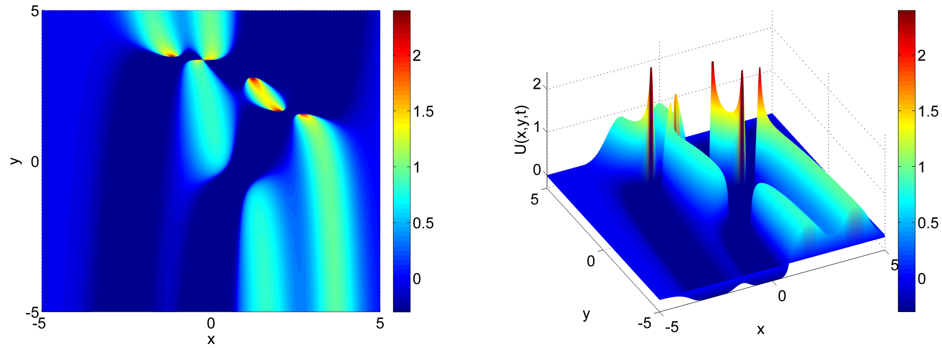


(a) Projection onto $xy$-plane

(b) 3D plot

Figure 3.27: Interaction of two singular waves with $\chi_1 = 2$, $\chi_2 = 2.5$, $\lambda_1 = 1.95$, $\lambda_2 = 1.65$, $\mu_1 = 0.006$, $\mu_2 = 0.01$, $\gamma_1 = 0.8$, $\gamma_2 = 1$, $\rho_1 = 3$, $\rho_2 = 0.3$, at $t = 0.1$.

All the graphs above were for the KPI equation. Now we look at graphs of the KPII equation, and see what effects surface tension and gravity have on the peaks of these waves. We start with the time evolution of the interaction of the singular waves of Figures 3.5 and 3.6 below.

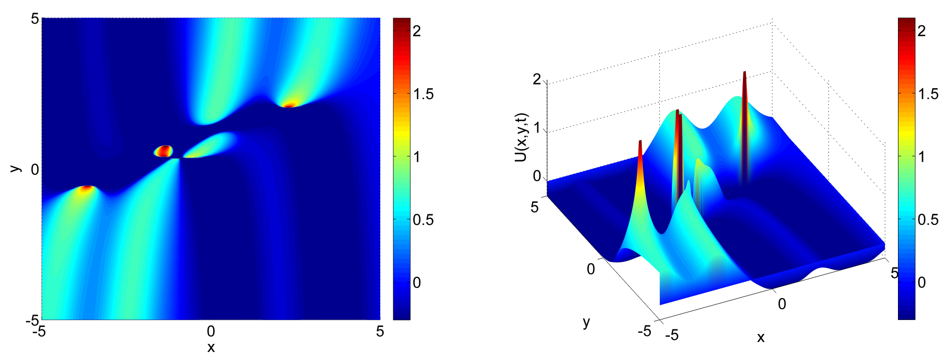


(a) Projection onto $xy$-plane

(b) 3D plot

Figure 3.28: Interaction of two singular waves with $\chi_1 = 1$, $\chi_2 = 2$, $\lambda_1 = 1.5$, $\lambda_2 = 1.3$, $\mu_1 = 0.01$, $\mu_2 = 0.009$, $\gamma_1 = \gamma_2 = 0$, $\rho_1 = \rho_2 = 0$, at $t = -0.1$.

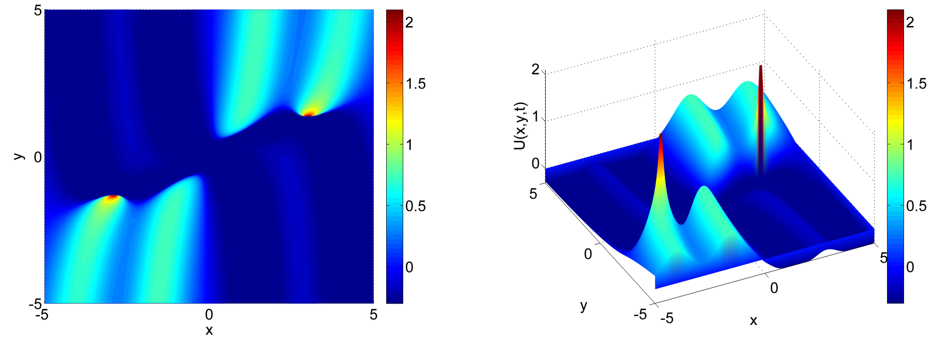


(a) Projection onto $xy$-plane (b) 3D plot

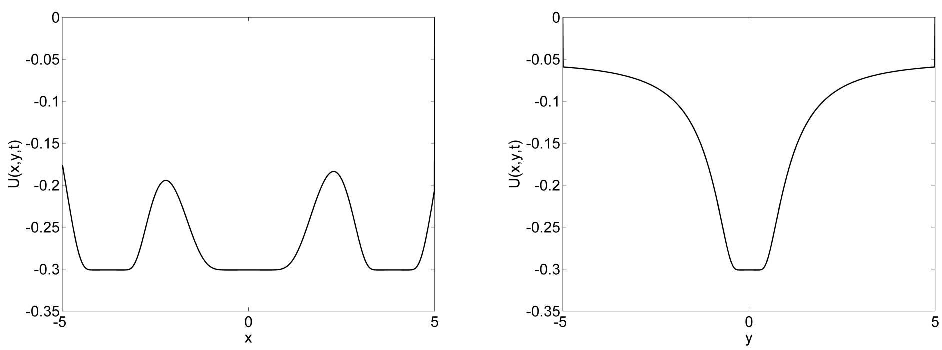


(c) Cross-Section by plane $y = 0$ (d) Cross-Section by plane $x = 0$

Figure 3.29: Interaction of two singular waves with $\chi_1 = 1$, $\chi_2 = 2$, $\lambda_1 = 1.5$, $\lambda_2 = 1.3$, $\mu_1 = 0.01$, $\mu_2 = 0.009$, $\gamma_1 = \gamma_2 = 0$, $\rho_1 = \rho_2 = 0$, at $t = 0$.

In the graphs for the KPI equation, we saw that the waves collided and energy accumulated to give birth to a new wave with an increased amplitude. This energy accumulation occurred at time $t = 0$. However, the graphs for the time evolution of the KPII equation (Figures 3.28, 3.29 and 3.30) show a different trend, where the energy accumulation is at time $t = 0.1$. We notice that, there are two peaks in Figure 3.29, however, these are considered unphysical, since they are not wide(strong) enough to stand alone.

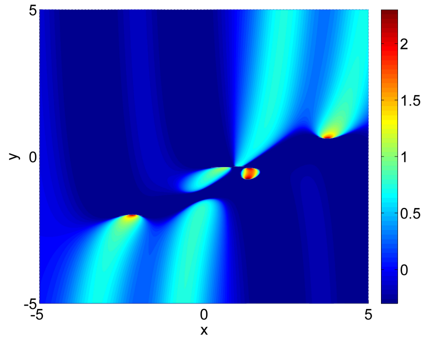


(a) Projection onto $xy$-plane

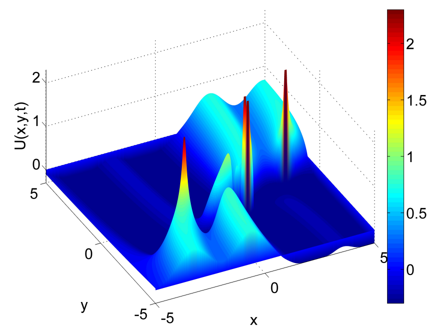


(b) 3D plot

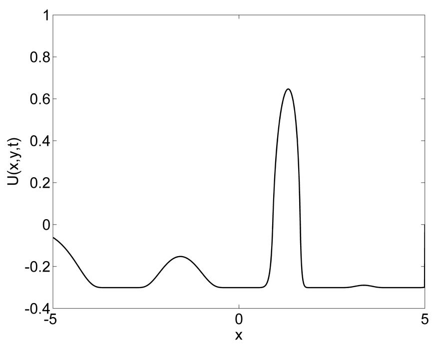


(c) Cross-Section by plane $y = 0$

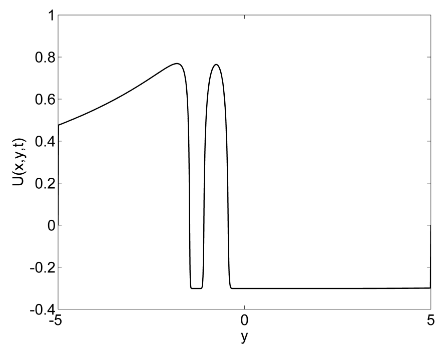


(d) Cross-Section by plane $x = 0$

Figure 3.30: Interaction of two singular waves with $\chi_1 = 1$, $\chi_2 = 2$, $\lambda_1 = 1.5$, $\lambda_2 = 1.3$, $\mu_1 = 0.01$, $\mu_2 = 0.009$, $\gamma_1 = \gamma_2 = 0$, $\rho_1 = \rho_2 = 0$, at $t = 0.1$.

The graphs in Figures 3.31-3.33 below, show another interesting case. Here, at time $t = 0$, Figure 3.32, we notice there is only one peak (increase in amplitude). This peak is not strong enough to support itself, so we consider it unphysical. At time $t = 0.1$, Figure 3.33, we observe two different peaks that are strong enough to support themselves. In this situation, we say the wave interaction did not produce a new wave of significant change in amplitude at time $t = 0$. However, at time $t = 0.1$, the interaction produced a new wave Figure 3.32, that is strong enough to support itself.

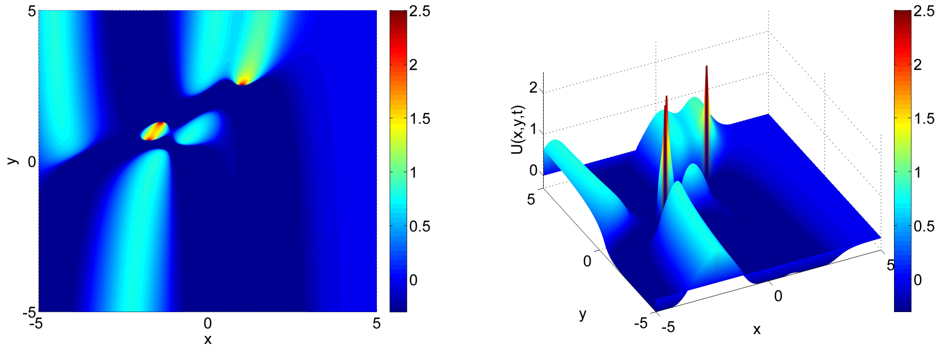


(a) Projection onto $xy$-plane (b) 3D plot

Figure 3.31: Interaction of two singular waves with $\chi_1 = 0.6$, $\chi_2 = 2$, $\lambda_1 = 1.5$, $\lambda_2 = 1.8$, $\mu_1 = 0.001$, $\mu_2 = 0.02$, $\gamma_1 = \gamma_2 = 0$, $\rho_1 = \rho_2 = 0$, at $t = -0.1$.

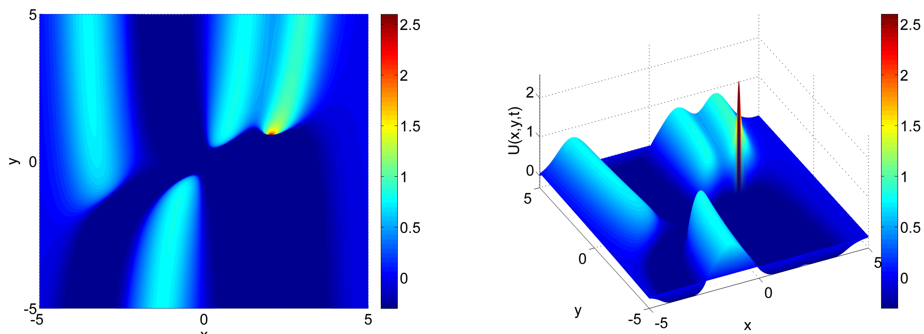


(a) Projection onto $xy$-plane (b) 3D plot

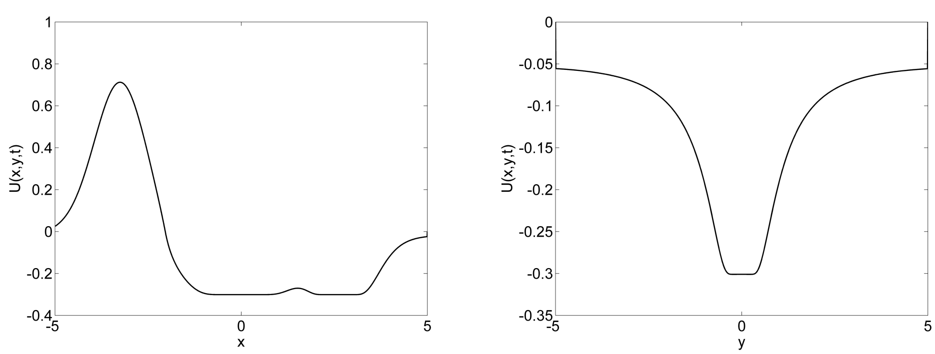


(c) Cross-Section by plane $y = 0$ (d) Cross-Section by plane $x = 0$

Figure 3.32: Interaction of two singular waves with $\chi_1 = 0.6$, $\chi_2 = 2$, $\lambda_1 = 1.5$, $\lambda_2 = 1.8$, $\mu_1 = 0.001$, $\mu_2 = 0.02$, $\gamma_1 = \gamma_2 = 0$, $\rho_1 = \rho_2 = 0$, at $t = 0$.

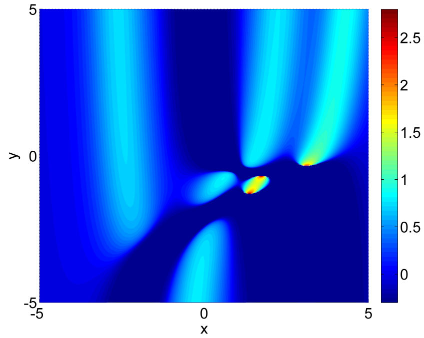


(a) Projection onto $xy$-plane

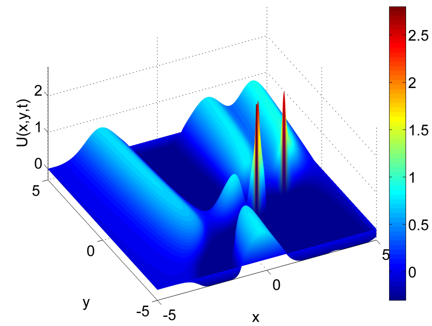


(b) 3D plot

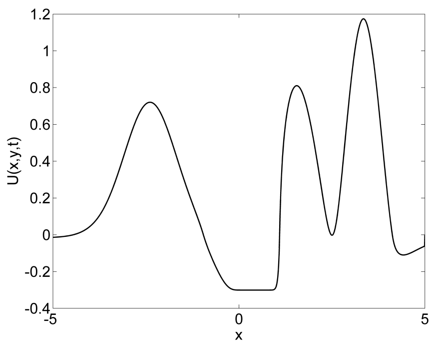


(c) Cross-Section by plane $y = 0$

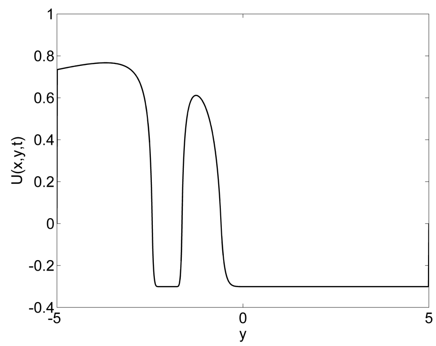


(d) Cross-Section by plane $x = 0$

Figure 3.33: Interaction of two singular waves with $\chi_1 = 0.6$, $\chi_2 = 2$, $\lambda_1 = 1.5$, $\lambda_2 = 1.8$, $\mu_1 = 0.001$, $\mu_2 = 0.02$, $\gamma_1 = \gamma_2 = 0$, $\rho_1 = \rho_2 = 0$, at $t = 0.1$.

The following graphs show the time evolution of the interaction of the singular waves of Figures 3.7 and 3.8. This graph has a similar trend to the graphs for the KPI equation, with a jump occurring at time $t = 0$, Figure 3.35. The only difference is that the jump that occurred at time $t = 0.1$, Figure 3.36 is bigger (taller) than that at time $t = 0$.

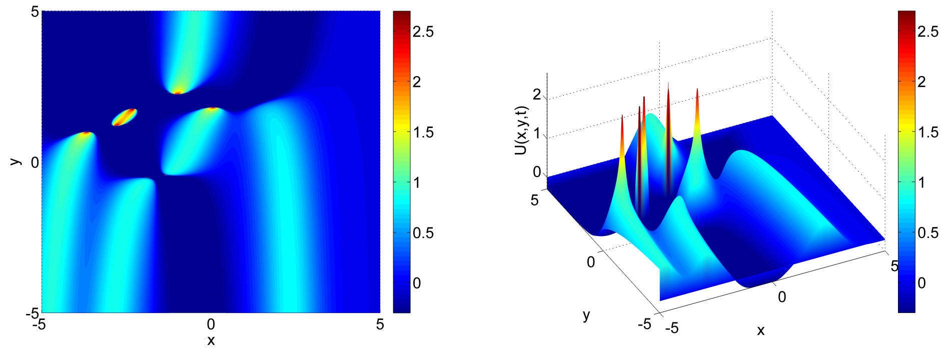


(a) Projection onto $xy$-plane (b) 3D plot

Figure 3.34: Interaction of two singular waves with $\chi_1 = 1.9$, $\chi_2 = 1.1$, $\lambda_1 = 1.7$, $\lambda_2 = 1.85$, $\mu_1 = 0.01$, $\mu_2 = 0.002$, $\gamma_1 = 0$, $\gamma_2 = 0.8$, $\rho_1 = 0.2$, $\rho_2 = 0$, at $t = -0.1$.

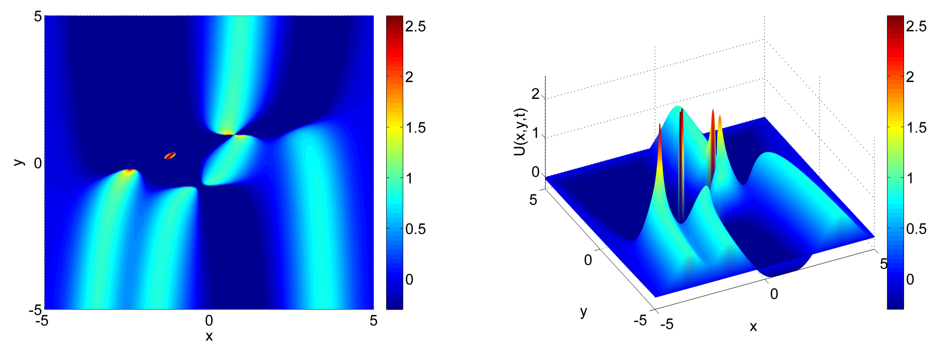


(a) Projection onto $xy$-plane (b) 3D plot

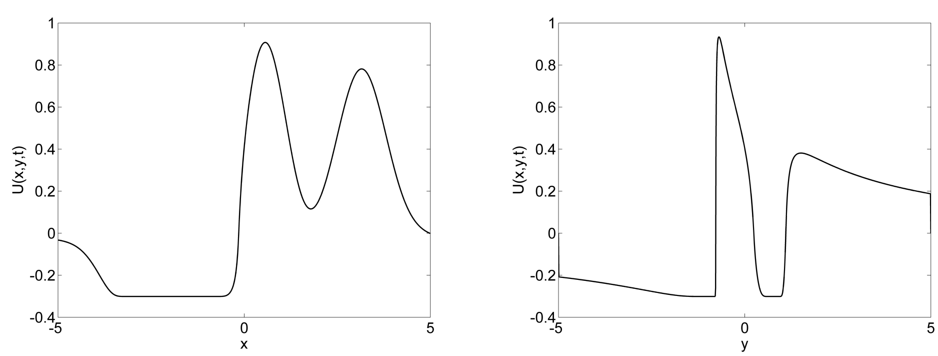


(c) Cross-Section by plane $y = 0$ (d) Cross-Section by plane $x = 0$

Figure 3.35: Interaction of two singular waves with $\chi_1 = 1.9$, $\chi_2 = 1.1$, $\lambda_1 = 1.7$, $\lambda_2 = 1.85$, $\mu_1 = 0.01$, $\mu_2 = 0.002$, $\gamma_1 = 0$, $\gamma_2 = 0.8$, $\rho_1 = 0.2$, $\rho_2 = 0$, at $t = 0$.

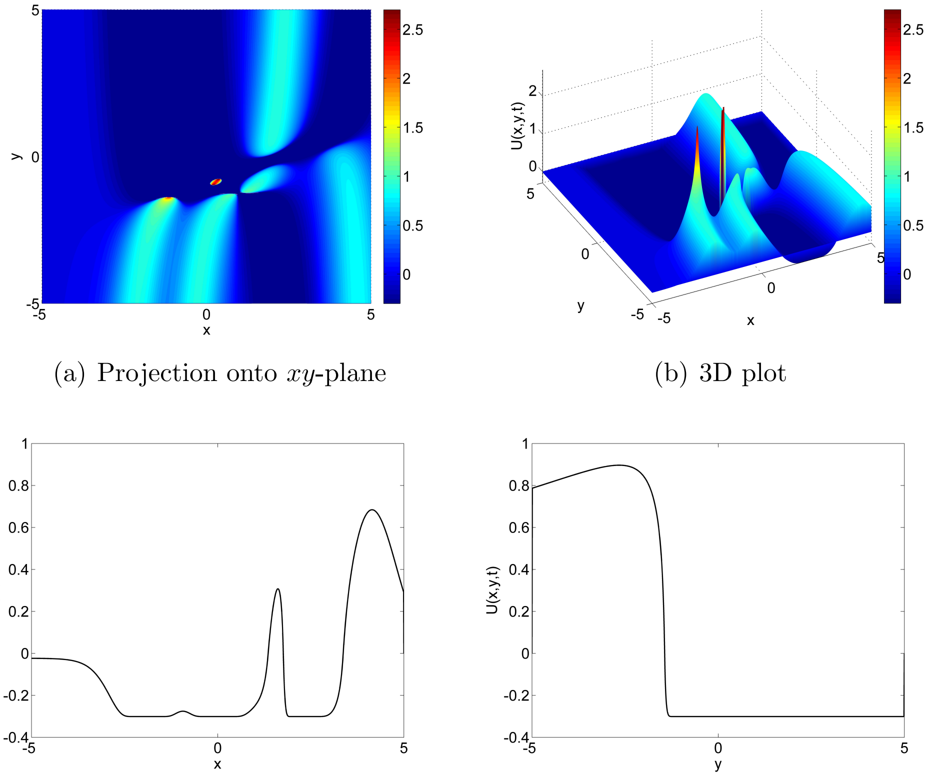


(a) Projection onto $xy$-plane (b) 3D plot

(c) Cross-Section by plane $y = 0$ (d) Cross-Section by plane $x = 0$

Figure 3.36: Interaction of two singular waves with $\chi_1 = 1.9$, $\chi_2 = 1.1$, $\lambda_1 = 1.7$, $\lambda_2 = 1.85$, $\mu_1 = 0.01$, $\mu_2 = 0.002$, $\gamma_1 = 0$, $\gamma_2 = 0.8$, $\rho_1 = 0.2$, $\rho_2 = 0$, at $t = 0.1$.

To conclude this section, we observe that the graphs of the KPI equation and KPII equations behave differently. Whilst all the graphs of the KPI equation shown here have the jumps and bigger waves occurring at time $t = 0$, the KPII equation had its bigger waves occurring at a later time, $t = 0.1$. We observe that, when surface tension dominates gravity (KPI equation), the jumps are bigger than when gravity dominates surface tension (KPII equation).

# Chapter 4

# Conclusion

The study and understanding of rogue waves is of great importance to us, because not only do they affect naval and civilian shipping, they can destroy coastal structures and offshore oil platforms. We can see such importance from the pictures that was taken from the Internet, Figure 4.2 at http://www.surfersvillage.com/news.asp?Id_news=14709, and Figure 4.1 at http://folk.uio.no/karstent/waves/index_en.html.

Figure 4.1: Destruction caused by a rogue wave - 1

Figure 4.2: Destruction caused by a rogue wave - 2

We used the Kadomtsev-Petviashvili equation to show the basic mechanism of rogue waves. Our solutions showed the appearance (occurrence) of large-amplitude waves with a short life span, that appear seemingly from nowhere and cause great destructions. We showed in particular how singular solutions (nonlinear waves) upon interaction suddenly create a new wave with an amplitude higher than those creating it, as a result of energy accumulation.

We must say that, the problem we considered is physical, however we did not take physical dimensions in our solutions. The solution obtained in this work is from the dimensionless form of the Kadomtsev-Petviashvili equation. As a result of this, contributions from physical parameters like wind, gravity, density and surface tension were lost.

We can conclude that, among the many theories for rogue waves, the mechanism produced by the Kadomtsev-Petviashvili model may be able to forecast and predict the occurrence of rogue waves. By studying the solutions obtained, the Kadomtsev-Petviashvili model seems to describe the time evolution of their interaction. Existing models say many waves come together and create rogue waves. In our study, we saw how two singular waves produced a wave with relatively high amplitude upon interaction. We also observed that even though the equation of our solution is dimensionless, the roles played by surface tension and gravity is evident. The amplitudes for solutions where surface tension dominates gravity were much higher than those where gravity dominates.

We observe that the Kadomtsev-Petviashvili model does not account for overturning waves. This is a limitation to the KP equation in modeling rogue waves, since these waves overturn at a point in their short life span. It should however be noted that, the KP equation can be quite a good model even under these 'ideal' conditions.

For further research, it will be interesting to see what to add to the KP equation to make it account for overturning waves and also for one to see the birth of these waves (i.e, total evolution of the wave). Also, we suggest that the physical KP equation be used in an experimental laboratory setting, with all the physical variables accounted for. This might go a long way in improving the results obtained in this thesis.

# Bibliography


[1] Ablowitz, M. J., Clarkson, P. A., Solitons, Non-Linear Evolution Equations and Inverse Scattering. *London Math. Society Lecture Notes*, Cambridge University Press, 1991.

[2] Bobenko, A. I., Bordag, L. A., Periodic multi-phase solutions of Kadomtsev-Petviashvili equation, *J. Phys. A*, **22**, no. **9**, 1259-1274, 1989.

[3] Boiti, M., Pempinelli, F., Pogrebkov, A. K., Some new methods and results in the theory of (2+1)-dimensional integrable equations, *Theoret. and Math. Phys.*, **99**, no. **2**, 511-522, 1994.

[4] Boiti, M., Pempinelli, F., Pogrebkov, A. K., Solving the Kadomtsev-Petviashvili equation with initial data not vanishing at large distances, *Inverse Problems*, **13**, no. **3**, L7-L10, 1997.

[5] Chow, K. W., Lai, W. C., Shek, C. K., Tso, K., Positon-like solutions of nonlinear evolution equations in (2+1) dimensions, *Chaos, Solitons and Fractals*, **9**, no. **11**, 1901-1912, 1998.

[6] Dodd, R. K., Eilbeck, J. C., Gibbon, J. D., Morris, H. C., Solitons and Nonlinear Wave Equations, *Academic Press*, 1982.

[7] Drazin, P. G., Johnson, R. S., Solitons: an introduction, *Cambridge University Press*, 1989.

[8] Hirota, R., Satsuma, J., N-soliton solutions of model equations for shallow water waves, *J. Phys. Soc. Japan*, **40**, no. **2**, 611-612, 1976.

[9] Infeld, E., Rowlands, G., Nonlinear Waves, Solitons and Chaos, *Cambridge University Press*, 2000.

[10] Kadomtsev, B. B., Petviashvili, V. I., On the stability of solitary waves in weakly dispersive media, *Sov. Phys. Dok.*, **15**, 539-543, 1970.

[11] Korteweg, D. J., de Vries, G., On the change of form of long waves advancing in a rectangular canal, and on a new type of long stationary waves, *Phil. Mag. (5)*, **39**, no. **240**, 422-443, 1895.

[12] Kovalyov, M., Slowly decaying solutions of KdV, *Contemporary mathematics*, **255**, 163-180, 2000.

[13] Kovalyov, M., Nonlinear interference and the Korteweg-de Vries equation, *Applied Mathematics Letters*, **9**, no. **5**, 89-92, 1996.

[14] Kovalyov, M., Hosseini Ali Abadi Mohammed, An explicit formula for a class of solutions of KdV, *Phys. Lett. A*, **254**, no. **1-2**, 47-52, 1999.

[15] Kovalyov, M., Basic motions of the Korteweg-de Vries equation, *Nonlinear Anal. Theory Methods Appl.*, **30**, no. **5/6**, 599-620, 1998.

[16] Kovalyov, M., On a class of KdV, *J. of Differential Equations*, **213**, no. **1**, 1-80, 2005.

[17] Kovalyov, M., Bica, I., Some properties of slowly decaying oscillatory solutions of KP, *Chaos, Solitons, and Fractals*, **25**, no. **5**, 979-989, 2005.

[18] Kundu, P. K., Cohen, I. M., Fluid Mechanics, *Academic Press*, 4th Ed., 2008.

[19] Manakov, S. V., Zakharov, V. E., Bordag, L. A., Its, A. R., and Matveev, V. B., Two-dimensional solitons of the Kadomtsev-Petviashvili equation and their interaction, *Phys. Lett.*, **63A**, 205-206, 1977.

[20] Müller, P., Garrett C. and Osborne, A., Rogue Waves, *Aha Huliko'a Hawaiian Winter Workshop, Oceanography*, **18**, no. **3**, 66-75, 2005.

[21] Novikov, S. P., Manakov, S. V., Pitaevskii, L. P., Zakharov, V. E., Theory of Solitons, The Inverse Scattering Method, *Contemporary Soviet Mathematics, Consultants Bureau, Plenum Publishing Corporation*, 1984.

[22] Russell, J. S., Report on waves, *Report of the Fourteenth Meeting of the British Association for the Advancement of Science*, York, 311, 1844.

[23] Satsuma, J., N-soliton Solution of the Two-dimensional Korteweg-de Vries Equation, *J. Phys. Soc. Japan*, **40**, 286-290, 1976.

[24] Whitham, G. B., Linear and Nonlinear Waves, *A Wiley-Interscience Publication*, John Wiley & Sons, 1974.

[25] Zabusky, N. S., Kruskal, M. D., Interaction of solitons in a collisionless plasma and the recurrence of initial states, *Phys. Rev. Lett.*, **15**, 240-243, 1965.

[26] Zeytounian, R. Kh., Nonlinear long waves on water and solitons, *Physics-Uspekhi*, **38**(12), 1333-1382, 1985.